*Acta Oceanol. Sin.*, 2024, Vol. 43, No. 11, P. 99–117
https://doi.org/10.1007/s13131-024-2431-7
http://www.aosocean.com
E-mail: ocean2@hyxb.org.cn

# The response of surface sedimental diatoms to the environment and its potential significance in the Taiwan Strait, western Pacific

Min Chen[1, 2, 3*], Xuan Liu[1, 2], Shuqin Tao[2, 3*], Aijun Wang[2, 3], Yanting Lin[1, 2], Zhaohe Luo[2], Ya Xu[2], Jiayu Li[2, 4], Qing Huang[2, 5]

[1] College of Marine Sciences, Shanghai Ocean University, Shanghai 201306, China

[2] Third Institute of Oceanography, Ministry of Natural Resources, Xiamen 361005, China

[3] Fujian Provincial Key Laboratory of Marine Physical and Geological Processes, Xiamen 361005, China

[4] College of Ocean and Earth Sciences, Xiamen University, Xiamen 361000, China

[5] School of Advanced Manufacturing, Fuzhou University, Jinjiang 362200, China

Received 28 February 2024; accepted 6 May 2024



**Abstract**

As the most important component of marine siliceous organisms, diatoms are vital primary producers of the ocean that are often used as indicators of paleoenvironmental change. To understand the response of sedimental diatoms to regional environmental changes and the factors affecting the distribution of sedimental diatoms in the Taiwan Strait, this study quantified and classified the diatoms found in surface sediments collected during four surveys from 2019 to 2020. Overall, 118 diatom taxa and 44 genera were identified with total diatom abundance of 8–27 353 valves/g. Four diatom assemblages representing different environments were identified. Among them, assemblage Ⅰ represented a coastal environment, assemblage Ⅱ comprised warm water species of a coastal environment, Assemblage Ⅲ represented a coastal environment affected markedly by exorheism, Assemblage Ⅳ represented a group with lowest diatom abundance. Seasonal variation in total diatom abundance was controlled by seven environmental factors: depth, sea surface salinity, mean grain size, silicate, nitrite, nitrate, and phosphate. Spatiotemporal variation in each of the diatom assemblages was substantial and strongly affected by various currents, upwelling, and low-salinity water. Specifically, it was found that the succession of diatom assemblages reflects change in the range of influence of local warm currents.

**Key words:** diatoms, surface sediments, current changes, Taiwan Strait

**Citation:** Chen Min, Liu Xuan, Tao Shuqin, Wang Aijun, Lin Yanting, Luo Zhaohe, Xu Ya, Li Jiayu, Huang Qing. 2024. The response of surface sedimental diatoms to the environment and its potential significance in the Taiwan Strait, western Pacific. Acta Oceanologica Sinica, 43(11): 99–117, doi: 10.1007/s13131-024-2431-7

## 1 Introduction

A diatom is a type of unicellular organism (Zhang, 2009). Diatoms are the most important component of marine siliceous organisms and they play a vital role in marine ecosystems (Ran et al., 2011). Diatoms are distributed widely in various water bodies around the world, and they are important providers of marine primary productivity, contributing approximately 40% of ocean primary productivity globally (Armbrust, 2009; Tréguer et al., 2018). There are many types of diatoms, and they are sensitive to environmental change (Chen et al., 2019), and they can quickly adapt to the water environment (Stoermer and Smol, 1999; Chen et al., 2022). Therefore, diatoms can be used as indicators of environmental change (Chen et al., 2020). The factors that control their distributions are often discussed by researchers when reconstructing both contemporary environments and paleoenvironments in paleoceanography and paleoclimatology studies (Chen et al., 2016; Edwards et al., 2006; Chang et al., 2009; Nakamura et al., 2020).

The Taiwan Strait is located off the southeast coast of China. On the western side of the Taiwan Strait, fresh water is discharged by the many large rivers, e.g., the Minjiang River and the Jiulong River. The region is strongly affected by the Asian monsoon, the hydrodynamic conditions are complex, and the ocean currents undergo frequent seasonal movement. Consequently, the Taiwan Strait is a region of land–sea interaction, and it represents a channel for the transport of material and energy in different marine environments. It also represents an important shallow water channel connecting the East China Sea and the South China Sea (Wang et al., 2016). The interaction between environmental changes and various environmental factors is intense. Therefore, the study of surface sedimental diatoms in the Taiwan Strait can provide rich information on regional paleocurrents and paleoclimate, and can revealing the evolution of regional paleoenvironment.

During the 1980s and 1990s, the common diatom genera and species in the Taiwan Strait were investigated and summarized (Jin et al., 1982). The absolute abundance and the dominant species of diatoms and silicoflagellates along the western coast of the Taiwan Strait were also studied (Lan, 1989), and how they were affected by currents, water depth, and sediments was discussed.

Foundation item: The Natural Science Foundation of Fujian Province of China under contract No. 2023J011378; the National Key Research and Development Program of China under contract No. 2019YFE0124700; the Special Fund for Basic Scientific Research Foundation of the Third Institute of Oceanography, Ministry of Natural Resources, China under contract Nos 2019018 and 2020017.
*Corresponding author, E-mail: chenmin@tio.org.cn; taoshuqin@tio.org.cn

It was later shown that ocean currents, temperature, salinity, and nutrient content drive the seasonal variations in the planktonic diatom community and abundance (Yang, 1995). In the early 21st century, the abundance and distribution of diatoms in the surface sediments in the upwelling area along the southeastern coast of Haitan Island in the northwest of the Taiwan Strait were explored (Fan et al., 2012), and it was identified that the highest abundance of sedimentary diatoms was in the center of the upwelling zone, reflecting the influence of upwelling on diatoms in the surface sediments. The proportions of benthic species and planktonic species in the western coastal waters of the Taiwan Strait were studied (Chen et al., 2012), and it was found that the proportion of benthic species was much larger than that of the other two types of diatoms. In winter and summer, the two sides of the Taiwan Strait are controlled by different currents that lead to differences in diatom subassemblages. The surface sedimental diatoms and columnar sedimental diatoms on the west side of the Taiwan Strait and their environmental significance were discussed (Mao, 2020). Studies on phytoplankton diatoms in certain areas of the Taiwan Strait have shown that phytoplankton diatoms are the most important part of the phytoplankton community in the Taiwan Strait, and that they are affected substantially by upwelling and nutrient limitation (Wang et al., 2016).

Few studies have investigated the continuous spatiotemporal variation of diatoms and the factors affecting the diatoms distribution in the surface sediments in the Taiwan Strait. Based on the sensitivity of diatoms to environmental changes, the response of spatiotemporal evolution of sedimental diatoms (from 2019 to 2020) to environmental changes and the main environmental factors controlling their distribution was studied. This study could be used to support the research of paleoenvironmental in the Taiwan Strait.

## 2 Study area

This study focused on the area in the west of the Taiwan Strait (Fig. 1). The Taiwan Strait is approximately 350-km long with average width of 180 km. The water depth is relatively shallow, i.e., the depth in over 75% of the strait is ⩽60 m (Xiao et al., 2002). The Taiwan Strait is in the southeastern margin of the Asian continent. The Taiwan Strait has SW-NE alignment (Liu et al., 2005; Hu et al., 2022). The Taiwan Strait has a subtropical marine climate that is affected substantially by the East Asian Monsoon. In winter and spring, the region is mainly affected by the northeast monsoon; in summer and autumn, it is mainly affected by the southwest monsoon from the ocean. Moreover, the area is affected frequently by tropical cyclones. Owing to the prevalence of the strong East Asian Monsoon, the flow in the Taiwan Strait is frequent throughout the year, and the ocean current system is highly seasonal. The surface circulation of the study area mainly includes the northward-flowing Taiwan Warm Current (TWC) as a branch of the Kuroshio Current, the Zhejiang-Fujian Coastal Current (ZMCC) system, and the East Guangdong Coastal Current from the SCS (Hong et al., 2009). The western side of the Taiwan Strait is affected most by the winter monsoon; thus, the ZMCC system is strong in winter (Zeng et al., 2021). During summer, a local zone of upwelling is formed in parts of the Taiwan Strait under the influence of the southwest summer monsoon (Hu et al., 2015). The seabed topography of the Taiwan Strait is

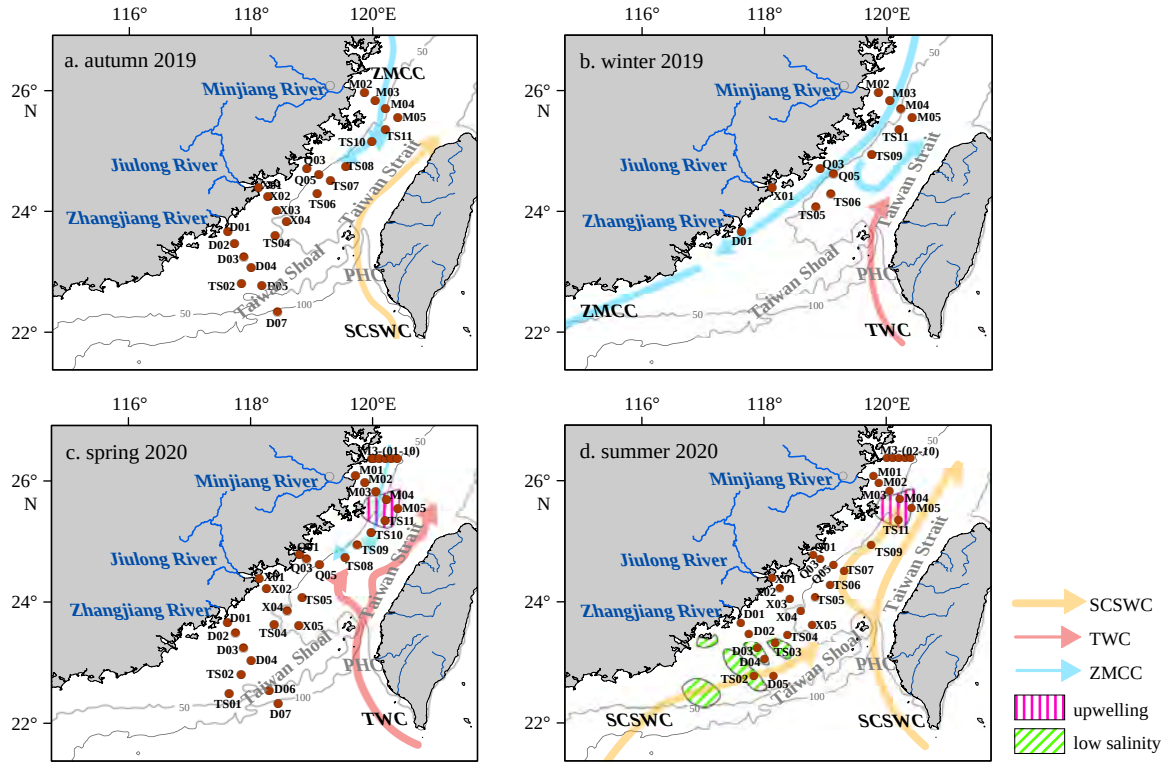


**Fig. 1.** Study area and locations of sampling stations (red dots): autumn 2019 (a), winter 2019 (b), spring 2020 (c), and summer 2020 (d). Red arrows represent the Taiwan Warm Current (TWC), blue arrows represent the Zhejiang-Fujian Coastal Current (ZMCC) system, and yellow arrows represent the South China Sea Warm Current (SCSWC) (Xiao et al., 2002; Sun, 2016; Tao et al., 2022). The thickness of each arrow indicates the strength of the current. Areas with green hatching represent zones of low sea surface salinity (Tang et al., 2002, 2004; Fan et al., 2012); areas with vertical purple lines represent areas with upwelling (Chen et al., 2008). The PHC represents Penghu Channel.

complex, i.e., it is generally high in the southwest and low in both the northeast and the southeast. It can be divided broadly into the central and western shoals of the Taiwan Strait, the Taiwan Strait Basin, the southern shoal of the Taiwan Strait (Taiwan Shoal), the Penghu Channel (PHC), and the submarine canyon (Hu, 2011). The PHC in the southeast is the deepest part, and represents the most important channel for the flow of the TWC from the Luzon Strait into the Taiwan Strait as a branch of the Kuroshio Current (Tao et al., 2022). The Taiwan Strait is located between the Asian continent and Taiwan Island. Its sediment sources include not only material transported from the East China Sea and the SCS, but also a large amount of terrigenous material derived from the Eurasian continent and regional alpine islands, which have a high erosion rate. The large–medium-sized rivers in Fujian Province on the western side of the Taiwan Strait, and the small–medium-sized rivers in Taiwan, discharge a large amount of sediment into the Taiwan Strait (Horng and Huh, 2011; Huh et al., 2011; Xu et al., 2013).

## 3 Methods

### 3.1 *Sample information*

For use in this study, samples of the uppermost 2 cm of the surface sediment in the Taiwan Strait were acquired using a grab sampler during surveys conducted in 2019 and 2020 by the Third Institute of Oceanography of the Ministry of Natural Resources, Xiamen (China). We collected 23 samples of surface sediment in autumn (October–November) 2019, 12 samples of surface sediment in winter (December) 2019, 32 samples of surface sediment in spring (May) 2020, and 31 samples of surface sediment in summer (August) 2020, i.e., a total of 98 samples from 4 consecutive seasons. The sedimentation rate in the study area is 0.4–2 cm/a (Xu et al., 1989; Huh et al., 2011). However, studies have shown that owing to the complex hydrodynamic conditions in the Taiwan Strait, the rate of sediment migration is faster and material can migrate to other regions within a period of 1–2 months (Milliman et al., 2007). Seasonal changes were found to have had impact on the multiyear mixed sediments.

### 3.2 *Diatom sample processing*

The processing and analysis of all diatom samples involved in this study were completed at the Third Institute of Oceanography. The modified Håkansso (1984) method was used to prepare the samples. Briefly, samples of approximately 5–15 g were dried in an oven at 60℃ and weighed before processing. Dry samples were treated with 10% HCL and 30% $H_2O_2$ to remove carbonates and organic material, and were then washed in distilled water to remove those chemicals from the solution. Samples were then soaked in distilled water for 24 h and scattered using an ultrasonic dispersion instrument (120 Hz) for 2 min. Most of the diatoms in the samples had diameter of >15 μm, which indicated that their relationship to the environment would be reliable. Similar studies showed that microdiatoms (<15 μm) have little influence on the results of such analyses (Chen et al., 2019) and therefore microdiatoms were not considered in this study. Each sample was placed in a 15-μm mesh sieve for filtration to remove microdiatoms and other material with diameter of <15 μm, and then the suspension containing the remaining diatoms was concentrated to 2–6 mL. When completely homogenized, 50 μL of the suspension was coated evenly on a cover glass (18 mm × 18 mm) and dried. Finally, three permanent slides were made for each sample using Canadian balsam as the fixative (Chen et al., 2020).

### 3.3 *Identification and counting of diatoms*

The diatoms on the sample slides prepared in this study were observed and identified using an Olympus BX51 optical microscope (objective lens: 40×, eyepiece: 20×). To be considered valid data, the number of diatoms in each sample should not be <300. For incomplete diatom valves, if the residual part of the valves was greater than half, it was included in the count. Classification and identification of the diatoms were based on various books and literature on diatom taxonomy (i.e., Jin et al., 1965, 1992; Jin, 1982; Cheng et al., 1996; Guo and Qian, 2003).

### 3.4 *Data processing and statistical methods*

To minimize the potential for error, we standardized the diatom data before conducting analysis. Genus organisms and characteristic species with relative percentage content of >2% were selected for further analysis; genus organisms that occurred at fewer than two stations were eliminated.

Figures drawing used ArcGIS 10.0.

In this study, absolute abundance and relative abundance were used to analyze the distribution characteristics of benthic diatoms. The absolute abundance of diatoms refers to the total number of diatoms per gram of dry sediment samples. The formula for calculating the absolute abundance of diatoms ($F$) is :

$$F = \frac{N}{W}, \tag{1}$$

where, $F$ is absolute abundance (valves/g); the total number of diatoms in $N$ is sample (number) ; $W$ is sample dry weight (g).

The relative abundance of diatoms refers to the percentage of each species in each sample to the total number of diatoms:

$$F' = \frac{F_i}{F_0}, \tag{2}$$

where, $F'$ is the relative abundance of each species (%) ; $F_i$ is the absolute abundance (valves/g) of each species ; $F_0$ is total diatom abundance (valves/g).

We used R software (package Vegan and version 3.5.2) to perform correlation and cluster analyses on both the diatom species data and the corresponding station environmental data. We determined the specific method of correlation analysis based on the variation range of the species data. Generally, if the range of species data are narrow, linear ordination methods are considered more applicable, e.g., redundancy analysis (RDA) and principal components analysis. When there is wide variation in the species data, single-peak models are generally selected, e.g., detrended correspondence analysis and canonical correspondence analysis (Ter Braak and Prentice, 1988). To determine the applicability of linear ordination methods and single-peak models to the data used in this study, we first performed detrended correspondence analysis on the species data, and obtained a gradient length of <3. Therefore, we considered that RDA was the most appropriate analysis method for this study.

To analyze the correlation between various environmental factors and diatom abundance, we used IBM SPSS 25 software, because of its simple operation and intuitive analysis of the Pearson correlation results.

### 3.5 *Environmental variables*

All environmental factor data involved in this study, derived from *in situ* measurements and laboratory tests, were obtained

from the basic database of the Special Fund for Basic Scientific Research Foundation of the Third Institute of Oceanography, State Oceanic Administration, China.

We chose mean grain size (Mz) as one of the environmental factors. Sediment Analysis of sediment particle size, including Mz, was performed using a MasterSizer2000 laser particle size analyzer at the Third Institute of Oceanography. The calculation was performed using the Folk–Ward rule (Folk and Ward, 1957).

Determination of nutrients was also completed at the Third Institute of Oceanography using a QuAAtro nutrient automatic analyzer [Marine Survey Specification–Marine Biological Survey (GB/T 12763.6-2007) and Marine Survey Specification–Marine Chemical Elements Survey (GB/T 12763.4-2007)]. Nitrate ($NO_3^-$-N) was determined using the pot column reduction method, nitrite ($NO_2^-$-N) was determined by ethylenediamine spectrophotometry, ammonia nitrogen ($NH_3$-N) was determined using the hypobromite oxidation method, phosphate ($PO_4^{3-}$-P) was determined by phosphorus blue extraction spectrophotometry, and active silicate ($SiO_3^{2-}$-Si) was determined using the silicon yellow method (Kang et al., 2020).

Other environmental factors such as sea surface temperature (SST), sea surface salinity (SSS), sampling water depth, dissolved oxygen (DO), and other data were measured using conductivity-temperature-depth probes (Seabird 19 plus).

The collection of all nutrient samples and the *in situ* measurement of all environmental factors were obtained at a depth of 5 m.

## 4 Results

### 4.1 *Environmental characteristics*

The overall variation in SSS in the study area (Fig. 2) was in the range of 27–35, gradually decreasing from the southeast to the northwest, with the same trend in autumn, winter, and spring. The influence of dilution by Minjiang River water was strong, and dilution by Jiulong River and Zhangjiang River water also had certain influence in spring. In summer, the overall SSS was high, and only slightly lower in river estuaries and the southern low-salinity SCS water intrusion. The seasonal difference of Mz (Fig. 3) in the study area was small. Coarse particles in autumn, spring, and summer were mainly distributed in the Taiwan Shoal. Because the sampling stations did not cover the Taiwan Shoal in winter 2019, coarse sediment particles in that season were found only along the coast, especially near Xiamen. Fine particles in the study area were mainly distributed in the northern Zhejiang–Fujian area of mud deposition (Liu et al., 2006). Except for winter 2019, sediment in the nearshore region of the study area predominantly comprised fine particles.

Except for phosphate, the contents of other nutrients in the study area vary greatly between seasons. The content of phosphate was low in all season. The content of silicate was higher in autumn and winter 2019, but lower in spring and summer 2020. The content of nitrite was higher in spring 2020, and the content of nitrate was higher in other seasons. The content of ammonia nitrogen was the highest in summer 2020. In terms of spatial distribution, the high value areas of phosphate, ammonia nitrogen, nitrate and silicate all appeared in Minjiang River and Jiulong River Estuary (Figs 4–8).

### 4.2 *Distribution of diatoms*

Overall, 118 taxa (including species and varieties) of 44 diatom genera were identified in the samples. Diatom abundance was in the range 8–27 353 valves/g. Diatom abundance changed substantially between the different seasons (Fig. 9). The range of diatom abundance in autumn 2019, winter 2019, spring 2020, and summer 2020 was 8–27 353 valves/g, 52–26 809 valves/g, 20–

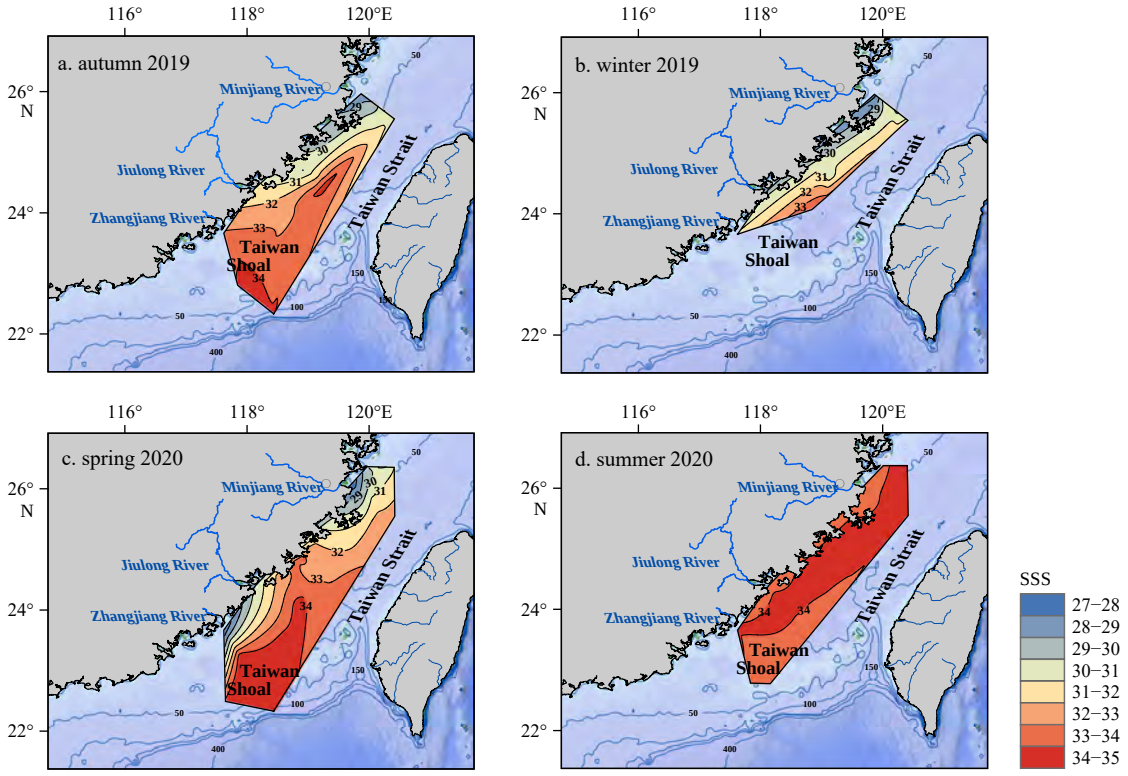


**Fig. 2.** Distribution of sea surface salinity (SSS) in the Taiwan Strait: autumn 2019 (a), winter 2019 (b), spring 2020 (c), and summer 2020 (d).

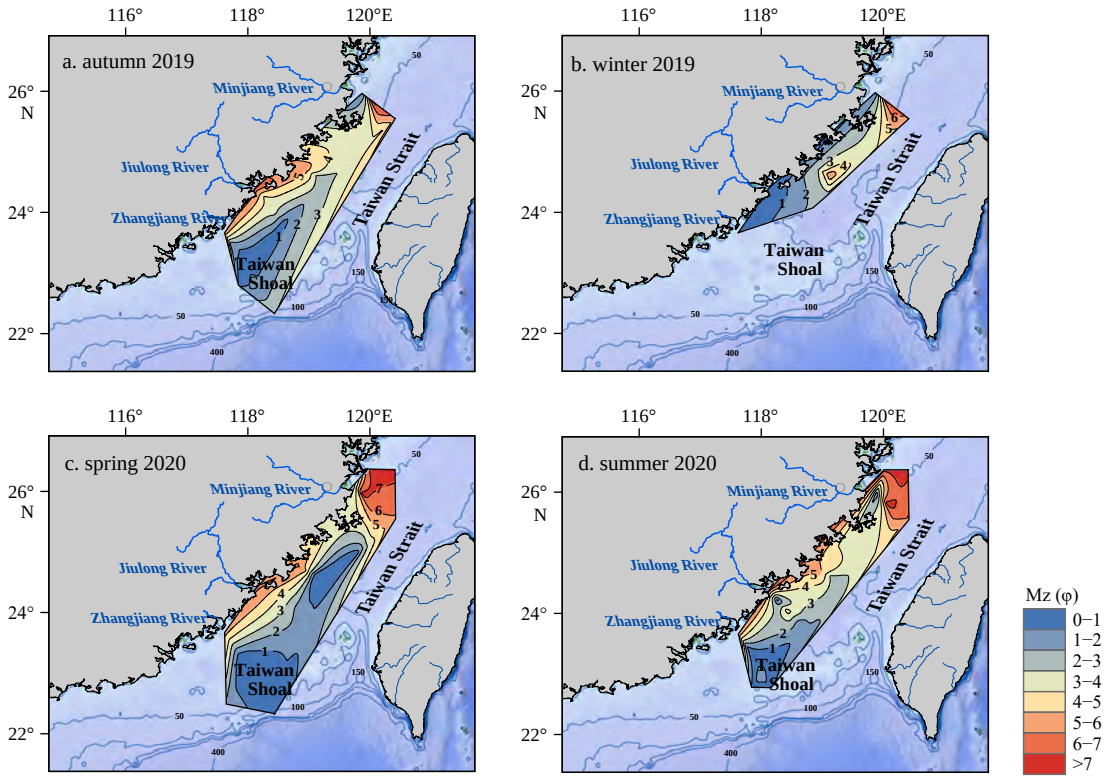


**Fig. 3.** Distribution of mean grain size (Mz) in the Taiwan Strait: autumn 2019 (a), winter 2019 (b), spring 2020 (c), and summer 2020 (d).

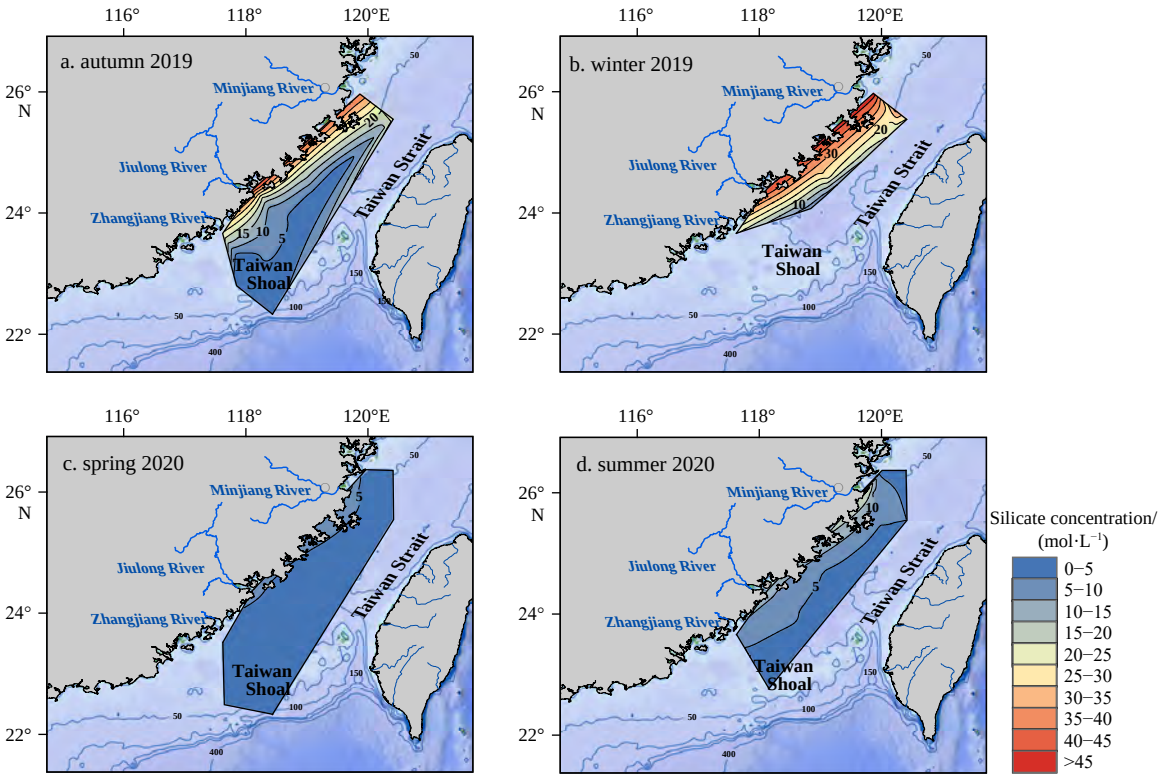


**Fig. 4.** Distribution of silicate in the Taiwan Strait: autumn 2019 (a), winter 2019 (b), spring 2020 (c), and summer 2020 (d).

14 651 valves/g, and 8–2 740 valves/g, respectively. Autumn 2019 had the largest variation in diatom abundance, while summer 2020 had the smallest variation. The total abundance of diatoms was highest in winter 2019, and lowest in summer 2020. The total abundance of diatoms in the four seasons was high along the western coast of the Taiwan Strait, decreasing eastward. At the same time, a secondary area of high values of diatom abundance was found in the north of the study area. In autumn and winter,

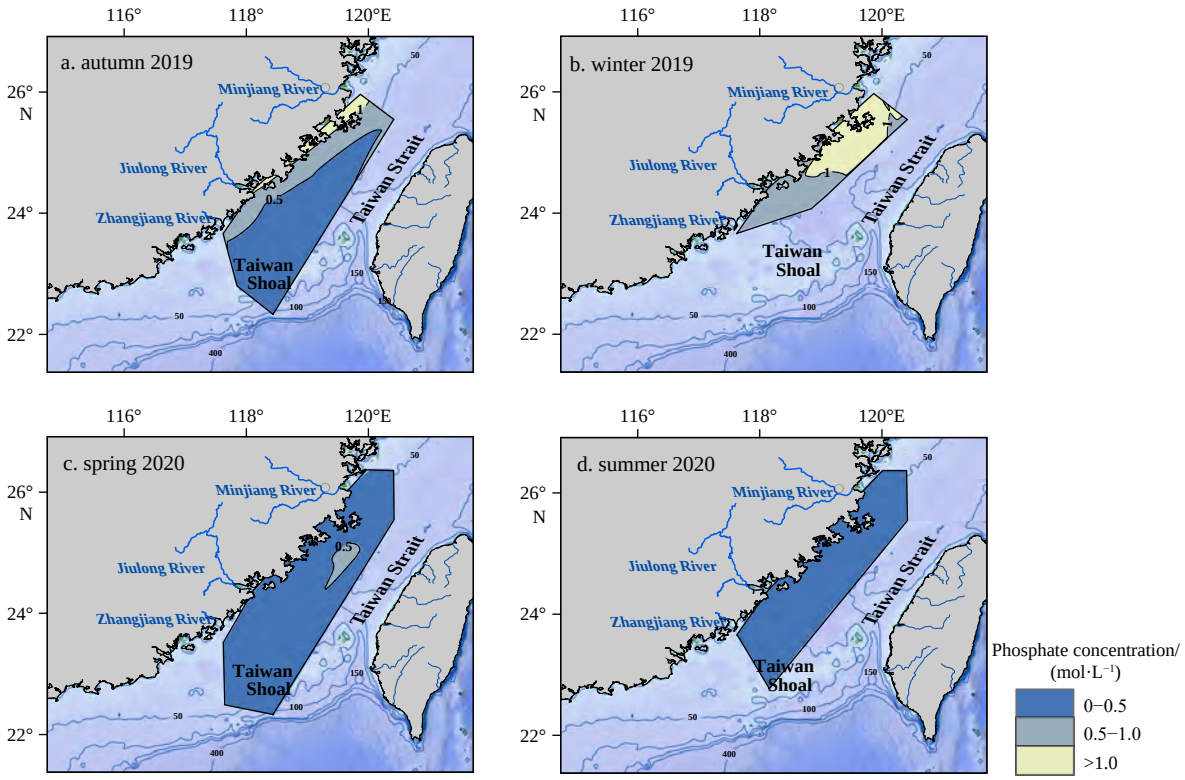


**Fig. 5.** Distribution of phosphate in the Taiwan Strait: autumn 2019 (a), winter 2019 (b), spring 2020 (c), and summer 2020 (d).

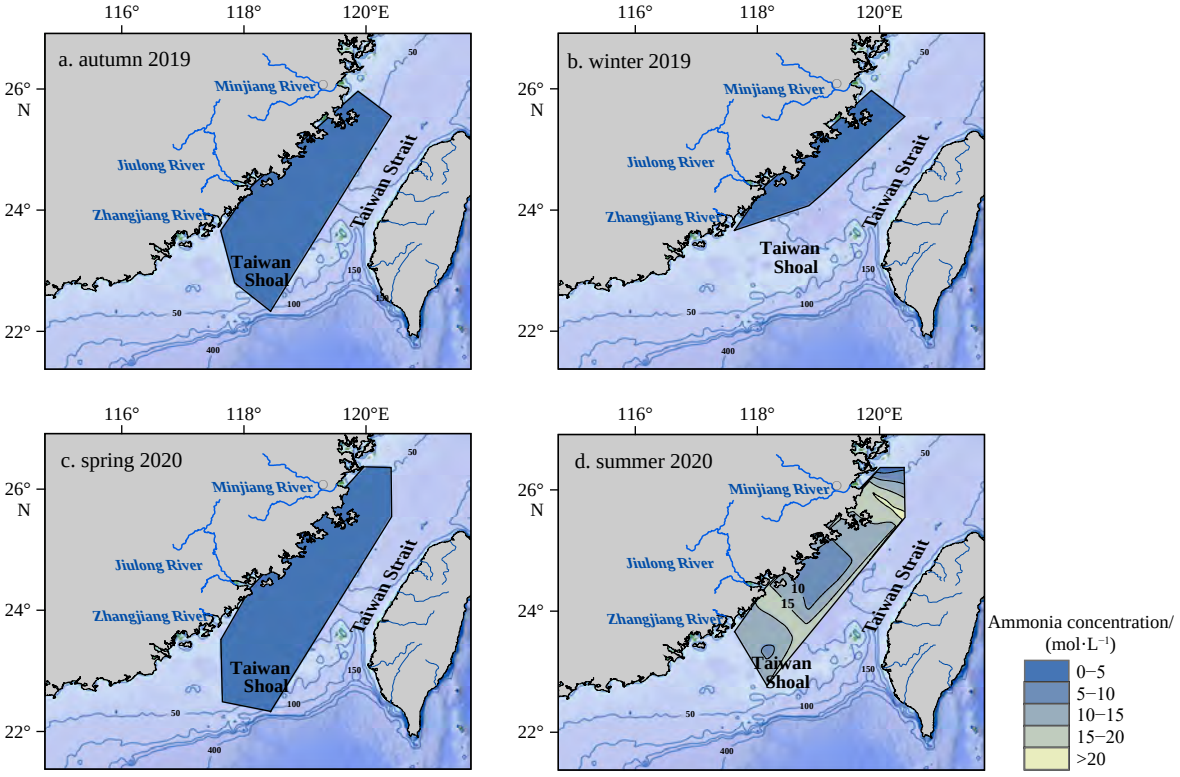


**Fig. 6.** Distribution of ammonia nitrogen in the Taiwan Strait: autumn 2019 (a), winter 2019 (b), spring 2020 (c), and summer 2020 (d).

diatom abundance in the western coastal region of the study area was the highest, especially in the area of the Jiulong River Estuary, where diatom abundance was >20 000 valves/g. In spring, the highest diatom abundance was distributed in the Zhangjiang River Estuary on the southwestern side of the study area.

This study used the relative percentage content of ⩾10% to determine the dominant species (Pokras and Molfino, 1986). Overall, 16 species were identified as dominant diatom species in

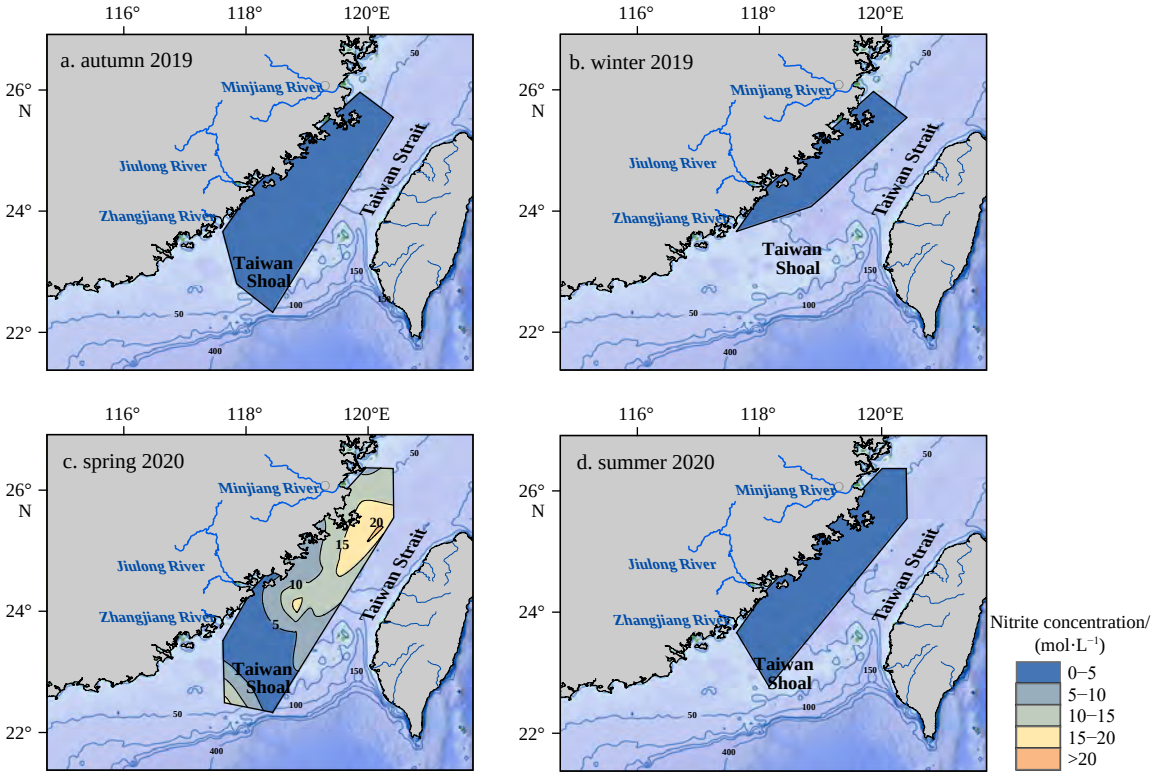


**Fig. 7.** Distribution of nitrite in the Taiwan Strait: autumn 2019 (a), winter 2019 (b), spring 2020 (c), and summer 2020 (d).

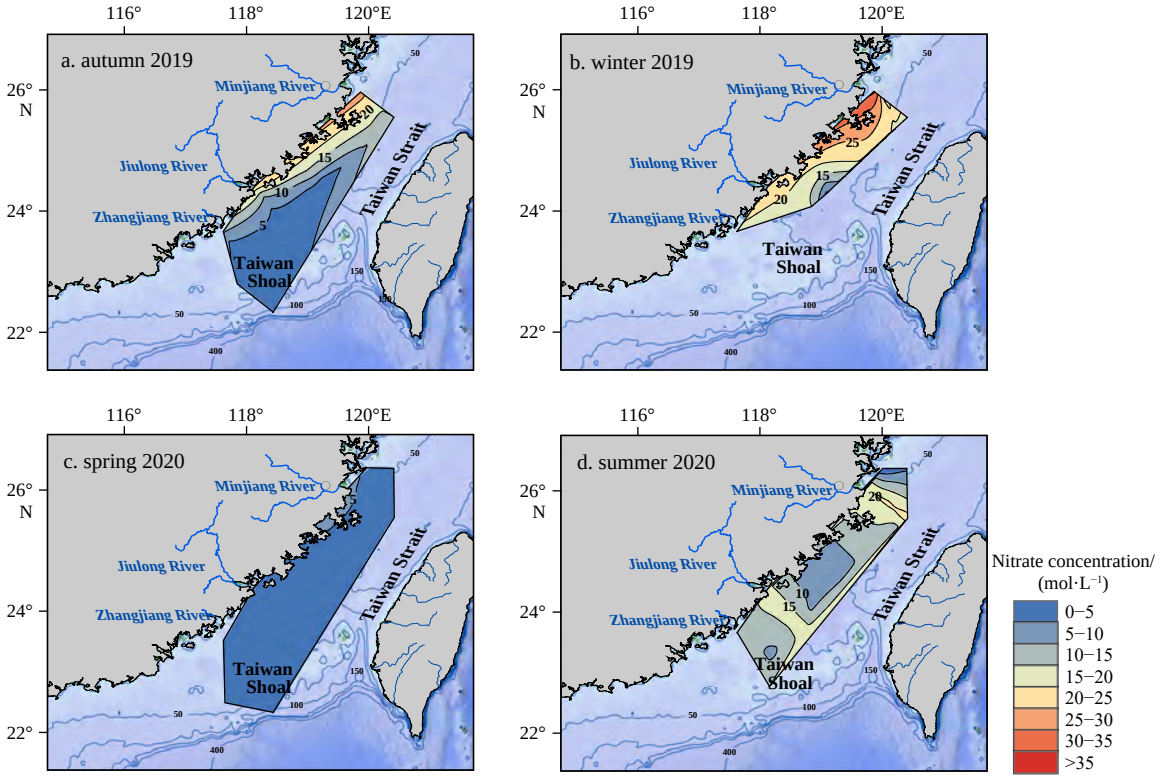


**Fig. 8.** Distribution of nitrate in the Taiwan Strait: autumn 2019 (a), winter 2019 (b), spring 2020 (c), and summer 2020 (d).

the four seasons in the study area (Table 1). The distribution of some dominant species was shown in Figs 10–13. The study area was dominated by marine species (Fig. 14) including *A. undulatus* (Fig. 13) , *C. radiatus* (Fig. 11) , *P. weyprechtii* and, etc., of which *Paralia sulcata* (Ehr.) Cleve (Fig. 10) had the highest content. However, there were also some brackish water species (Fig. 15) including *C. stylorum*, *Nitzschia obtusa var. scalpelliformis* Grunow, *Nitzschia sigma* (Kützing) W.Smith, *Nitzschia lorenziana*

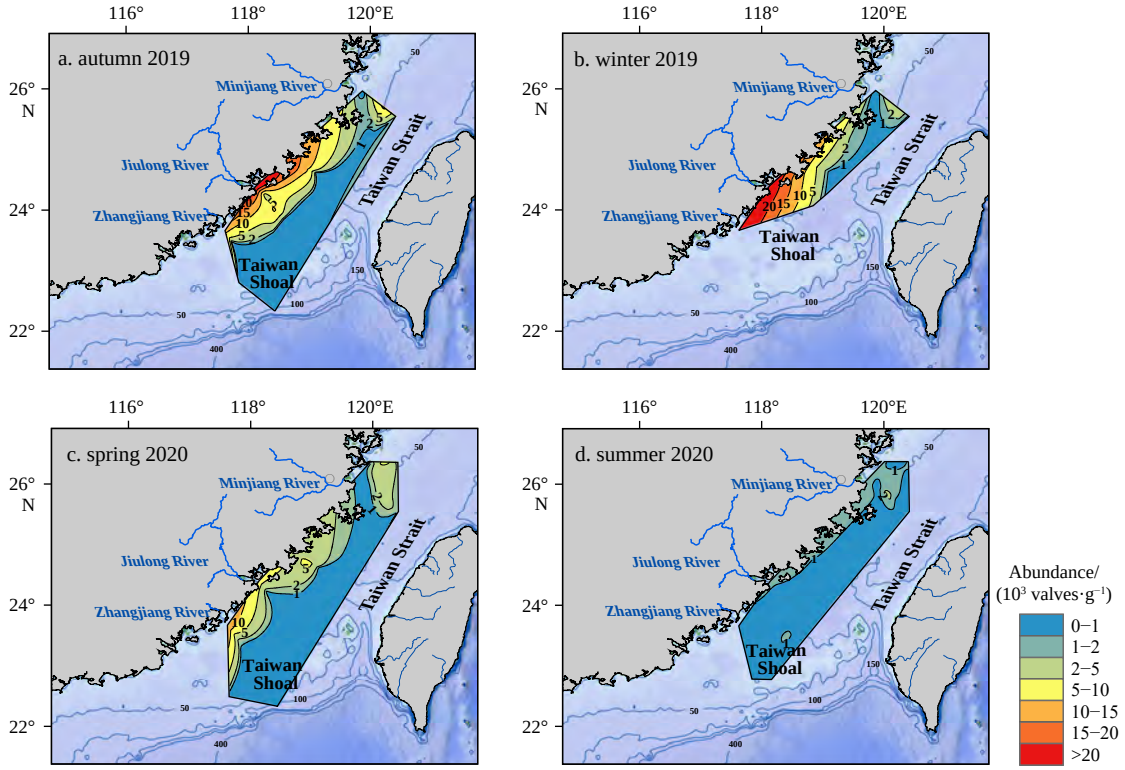


**Fig. 9.** Distribution of diatom abundance in the Taiwan Strait: autumn 2019 (a), winter 2019 (b), spring 20202 (c), and summer 2020 (d).

Grunow, *Achnanthes hauckiana* Grunow, etc., and *Coscinodiscus rothii* (Ehrenberg) Grunow (Fig. 12) had a higher content at some stations. Freshwater species appeared only sporadically including *Cyclotella meneghiniana* Kiitzing, *Diploneis elliptica* (Kützing) Cleve, *Melosira granulata* (Ehrenberg) Ralfs, *Cymbella tumida* (A. Schmidt) Skabichevskii, etc. Additionally, the content of warm water species was relatively high (Fig. 16), especially that of *Azpeitia nodulifera* (Schimidt) Fryxell and Sims.

### 4.3 *Characteristics of diatom assemblages*

To determine the spatiotemporal changes of diatom assemblages in the study area, we integrated the diatom data for the four seasons for further analysis. Overall, 98 diatom species with relative percentage content of >2% and occurrence at two or more stations were selected. To ensure that the analysis accurately reflected the ecological characteristics of the diatom communities, we also included the rare species of freshwater species, warm water species, and other characteristic species of diatoms in the analysis. The freshwater species we selected mainly included *Cyclotella comta* (Ehr.) Kützing, *Aulacoseira granulata* (Ehr.) Simonsen, and *C. meneghiniana*. The warm water species mainly included *A. nodulifera*, *Campylodiscus brightwellii* Grunow and *Azpeitia africanus* Janisch. Environmental data included depth, Mz, SSS, SST, DO, silicate (Si), ammonia nitrogen ($NH_3$), phosphate ($PO_4^{3-}$), nitrite ($NO_2^-$), and nitrate ($NO_3^-$).

Owing to a lack of environmental data for some stations, we selected only those 71 stations that had complete environmental data for RDA. The results of RDA between the environmental variables and stations and between the environmental variables and species are shown in Figs 17–18 and Table 2, respectively. Additionally, the samples were divided into four diatom assemblages and a special case station following cluster analysis (Figs 17 and 18).

#### 4.3.1 *Diatom assemblage* Ⅰ*: P. sulcata-A. undulatus-C. oculatus-P. weyprechtii-P. stelliger-C. radiatus*

Assemblage I was dominated by coastal and benthic species, namely *A. undulatus*, *P. sulcata*, and *P. stelliger* with average content of 6.88%, 27.08%, and 5.84%, respectively (Table 3). There were also planktonic species *C. oculatus*, *C. radiatus*, and *P. weyprechtii* with content of 6.70%, 4.95%, and 6.38%, respectively (Table 3). The total diatom abundance in this assemblage was the highest (range: 236–27 353 valves/g, average: 4 028 valves/g) in comparison with that of the other assemblages. Assemblage Ⅰ was positively correlated with nutrients and depth and negatively correlated with SST (Fig. 17). The assemblage was widely distributed in the other three seasons, except it showed a reduction in summer 2020 (Fig. 19). In autumn 2019, the assemblage was mainly distributed in the sea area extending outward from the estuaries of the Minjiang River, Jiulong River, and Zhangjiang River. In winter 2019, the distribution extended along the entire coast. In spring 2020, the assemblage was also distributed in the sea area extending outward from the estuaries of the Minjiang River, Jiulong River, and Zhangjiang River, but additionally at some stations to the north of the Minjiang River Estuary. In summer 2020, the number of stations on the eastern side of the study area at which Assemblage Ⅰ was distributed decreased markedly, and the assemblage was found mainly distributed in the western nearshore area. Overall, diatom Assemblage Ⅰ most likely represents a coastal group.

#### 4.3.2 *Diatom assemblage* Ⅱ*: C. rothii-P. sulcata-C. striata-P. stelliger-A. nodulifera-Trachyneis sp.*

Assemblage Ⅱ comprised the most common coastal species such as *C. rothii, C. striata*, *P. sulcata*, and *P. stelliger*, but it also contained a common warm water diatom species *A. nodulifera*, the content of which was 23.5%, 7.78%, 9.05%, 7.69%, and 3.67%,

**Table 1.** Dominating diatom species (relative abundance > 10%) in the surface sediment in the study area

| Season | Number of genera | Number of taxa | Dominating species | Abundance range/% | Average abundance/% |
|---|---|---|---|---|---|
| Autumn 2019 (October–November) | 31 | 71 | *Actinoptychus undulatus* (Bail.) Ralfs | 0–13.51 | 3.50 |
| | | | *Coscinodiscus divisus* Grunow | 0–10.77 | 0.82 |
| | | | *Coscinodiscus oculatus* (Fauv.) Petit | 0–14.66 | 2.78 |
| | | | *Coscinodiscus radiatus* Ehrenberg | 0–28.57 | 3.85 |
| | | | *Coscinodiscus rothii* (Ehr.) Grunow | 0–70.77 | 5.08 |
| | | | *Paralia sulcata* (Ehr.) Cleve | 0–64.18 | 28.57 |
| | | | *Pyxidicula weyprechtii* Grunow | 0–15.38 | 3.67 |
| | | | *Trachyneis aspera* (Ehrenberg) Cleve | 0–10.81 | 1.97 |
| Winter 2019 (December) | 30 | 62 | *Actinoptychus undulatus* (Bail.) Ralfs | 0–13.51 | 3.92 |
| | | | *Coscinodiscus radiatus* Ehrenberg | 0–10.77 | 1.24 |
| | | | *Cyclotella stylorum* Brightwell | 0–14.66 | 3.27 |
| | | | *Paralia sulcata* (Ehr.) Cleve | 0–28.57 | 4.88 |
| | | | *Podosira stelligera* (Bail.) A.Mann | 0–70.77 | 7.81 |
| | | | *Pyxidicula weyprechtii* Grunow | 0–64.18 | 30.05 |
| Spring 2020 (May) | 33 | 92 | *Actinoptychus undulatus* (Bail.) Ralfs | 0–36.26 | 7.87 |
| | | | *Coscinodiscus curvatulus var.minor* (Ehr.) Grunow | 0–40.87 | 2.27 |
| | | | *Coscinodiscus decrescens* Grunow | 0–12.26 | 1.31 |
| | | | *Coscinodiscus oculatus* (Fauv.) Petit | 0–31.11 | 7.98 |
| | | | *Coscinodiscus radiatus* Ehrenberg | 0–18.37 | 4.23 |
| | | | *Cyclotella stylorum* Brightwell | 0–10.32 | 1.64 |
| | | | *Paralia sulcata* (Ehr.) Cleve | 0–53.19 | 16.39 |
| | | | *Podosira stelligera* (Bail.) A.Mann | 0–50 | 6.59 |
| | | | *Pyxidicula weyprechtii* Grunow | 0–26.67 | 5.13 |
| | | | *Thalassiosira pacifica* Gran & Angst | 0–11.63 | 2.79 |
| Summer 2020 (August) | 26 | 60 | *Actinocyclus ehrenbergii* Ralfs | 0–11.76 | 1.76 |
| | | | *Actinoptychus undulatus* (Bail.) Ralfs | 0–16.67 | 3.33 |
| | | | *Biddulphia tuomegi*(Bail.)Roper | 0–18.75 | 1.39 |
| | | | *Coscinodiscus oculatus* (Fauv.) Petit | 0–33.33 | 4.13 |
| | | | *Coscinodiscus rothii* (Ehr.) Grunow | 0–100 | 10.75 |
| | | | *Cyclotella striata* (Kützing) Grunow | 0–100 | 5.72 |
| | | | *Cyclotella stylorum* Brightwell | 0–23.53 | 2.65 |
| | | | *Paralia sulcata* (Ehrenberg) Cleve | 0–100 | 29.90 |
| | | | *Podosira stelligera* (Bail.) A.Mann | 0–42.86 | 7.84 |
| | | | *Pyxidicula weyprechtii* Grunow | 0– 100 | 9.15 |

respectively. Additionally, the freshwater species *C. meneghiniana*, which appeared in this assemblage with content of 1.94%, was distributed at Stations D04 and D07 in spring 2020. The total diatom abundance in this assemblage was low (range: 12–163 valves/g, average: 58 valves/g). This assemblage was positively correlated with SST, SSS, and $NH_3$ and negatively correlated with depth (Fig. 17). Assemblage Ⅱ was mainly distributed in the Taiwan Shoal area in autumn 2019, spring 2020, and summer 2020. In the spring and summer of 2020, Assemblage Ⅱ was found distributed at a few stations in central and northern parts of the study area, but the assemblage was missing in winter 2019 (Fig. 19). Overall, Assemblage Ⅱ represented a coastal group including warm water species.

4.3.3 *Diatom assemblage* Ⅲ*: P. sulcata-P. weyprechtii-P. stelliger-C. rothii*

Assemblage Ⅲ comprised mainly marine benthic species, including *P. sulcata* and *P. stelliger* with content of 34.92% and 8.87%, respectively. The planktonic species *C. rothii* and *P. weyprechtii* were also found in this assemblage, with content of 3.63% and 12.26%, respectively, among which *P. weyprechtii* was an exotic species. The typical shallow marine species *P. sulcata* had the highest content, and those stations with higher content were in water with depth in the range of 50–100 m, consistent with the findings of previous studies (Zhang et al., 2016; Jiang, 1987; Wang et al., 1990). The total diatom abundance in this assemblage was 8–244 valves/g (average: 115 valves/g). This assemblage was positively correlated with SSS, SST, and depth and negatively correlated with Mz (Fig. 17). The total number of stations at which Assemblage Ⅲ was found was second only to the total number of stations at which Assemblage Ⅰ was found. In autumn 2019, the assemblage was mainly distributed in the outer sea side of the north–central part of the study area. In winter 2019 and spring 2020, the assemblage was less well distributed. In summer 2020, the assemblage was mainly distributed in the outer extension of the Minjiang River Estuary, along the central coast, and in the open sea of the study area; it was also found at two stations in the Taiwan Shoal area (Fig. 19). This assemblage represented a coastal shallow water environment affected by the oceanic water.

4.3.4 *Diatom assemblage* Ⅳ*: T. eccentrica-C. decrescens*

Assemblage Ⅳ comprised *C. decrescens* and *Thalassiosira eccentrica* Karsten with content of 25% and 50%, respectively. The total diatom abundance of this assemblage was the lowest (range: 8–38 valves/g, average: 23 valves/g). This assemblage was positively correlated with SSS and $NH_3$ and negatively correlated

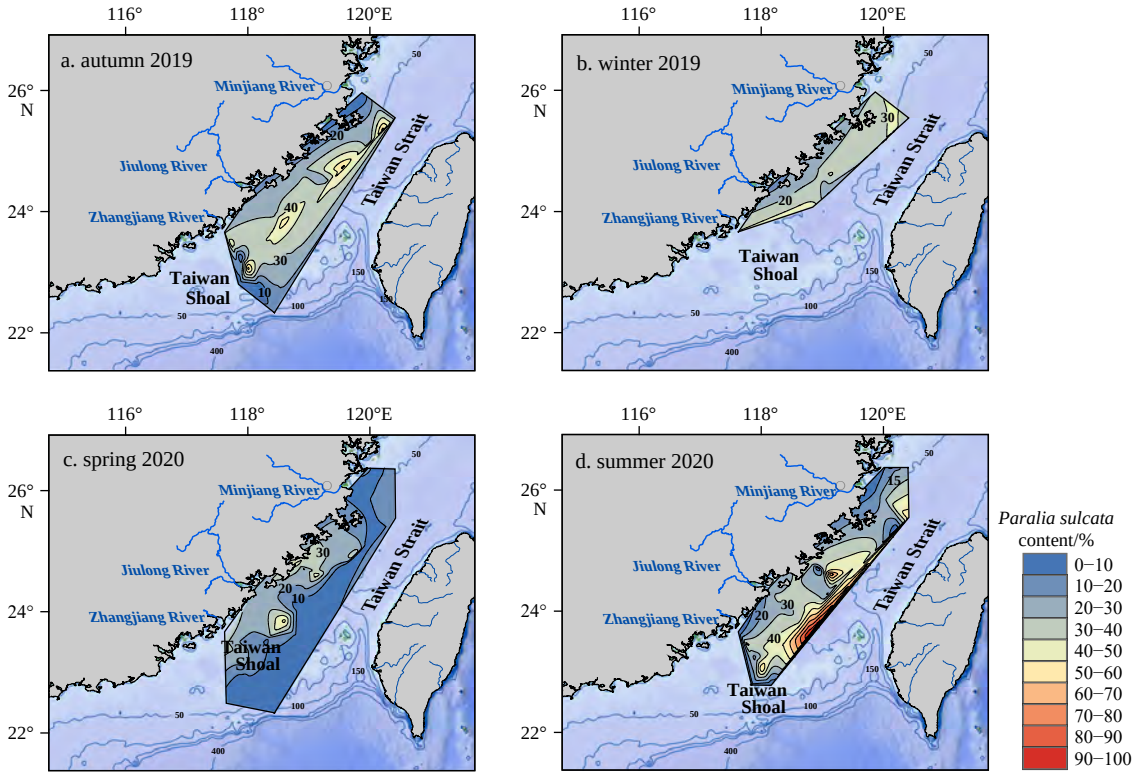


**Fig. 10.** Distribution of *Paralia sulcata* in the Taiwan Strait: autumn 2019 (a), winter 2019 (b), spring 2020 (c), and summer 2020 (d).

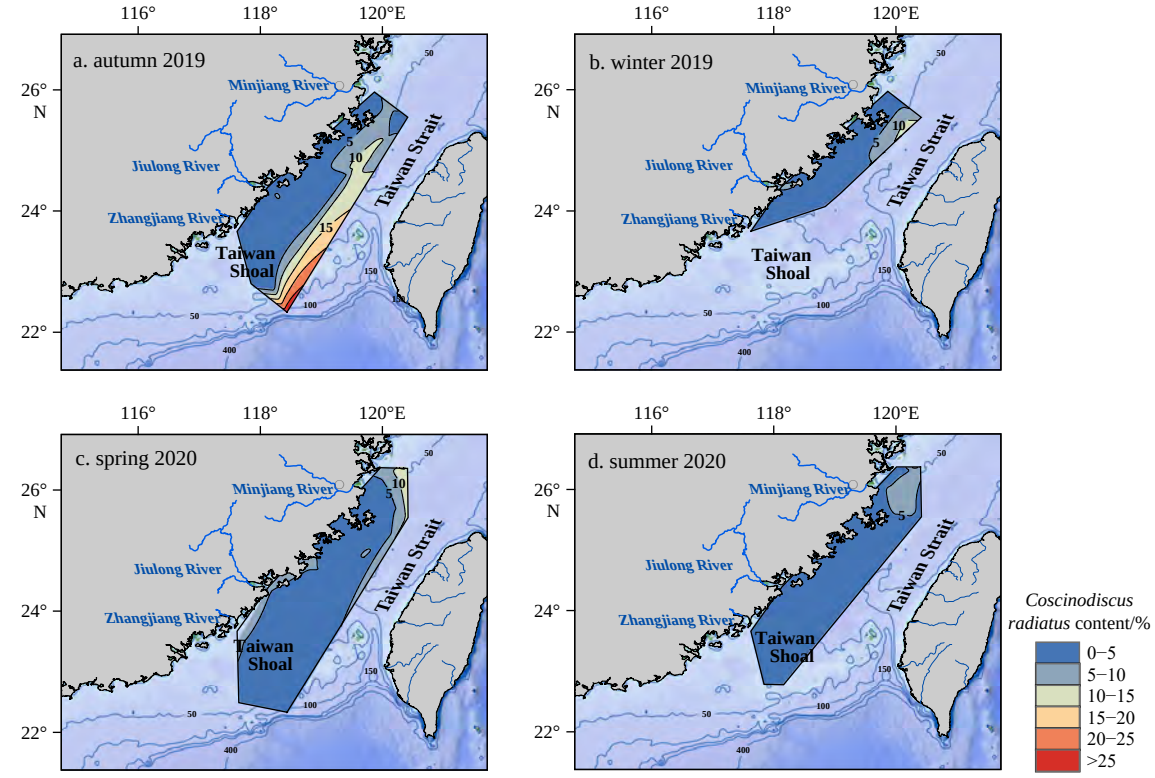


**Fig. 11.** Distribution of *Coscinodiscus radiatus* in the Taiwan Strait: autumn 2019 (a), winter 2019 (b), spring 2020 (c), and summer 2020 (d).

with depth, Mz, and nutrients (Fig. 17). Assemblage Ⅳ was mainly distributed at Station M02 in the Minjiang River Estuary in autumn 2019 and at Station TS11 to the south of the Minjiang River Estuary in summer 2020 (Fig. 19).

4.3.5 *Other*

We also precipitated a separate group (Station TS05) in spring 2020 following cluster analysis. The abundance at TS05 was very low, i.e., approximately 20 valves/g, and the diatoms included *A.*

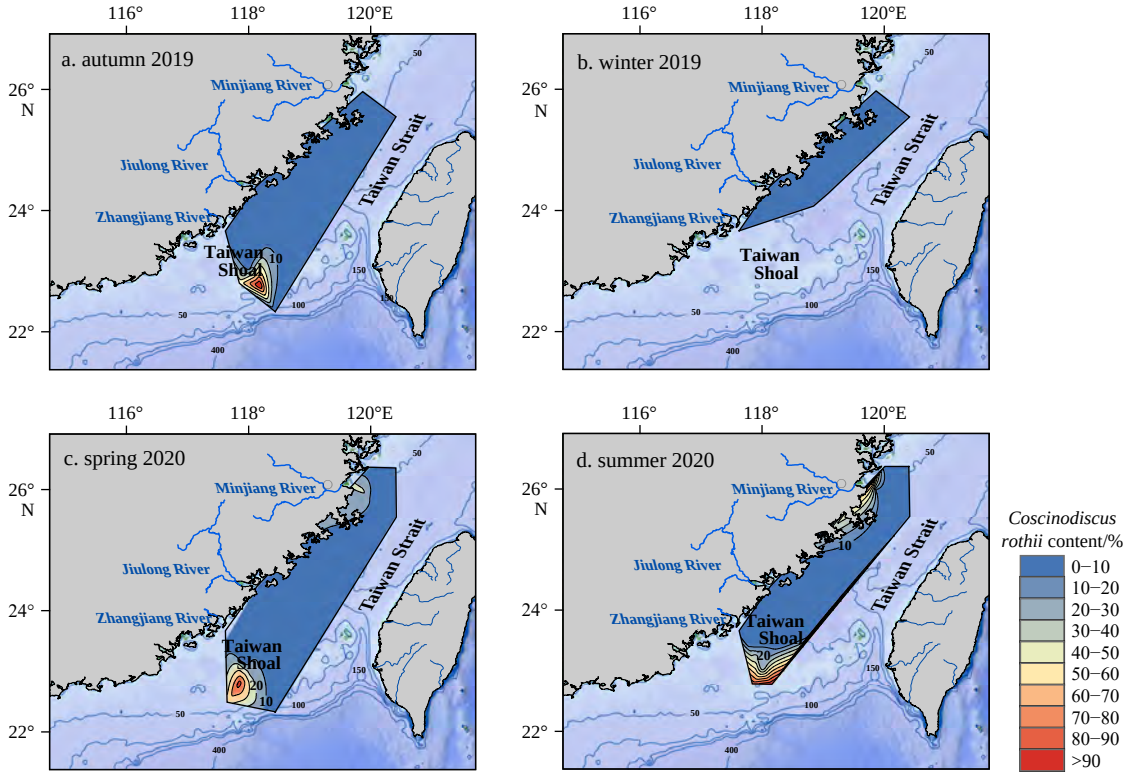


**Fig. 12.** Distribution of *Coscinodiscus rothii* in the Taiwan Strait: autumn 2019 (a), winter 2019 (b), spring 2020 (c), and summer 2020 (d).

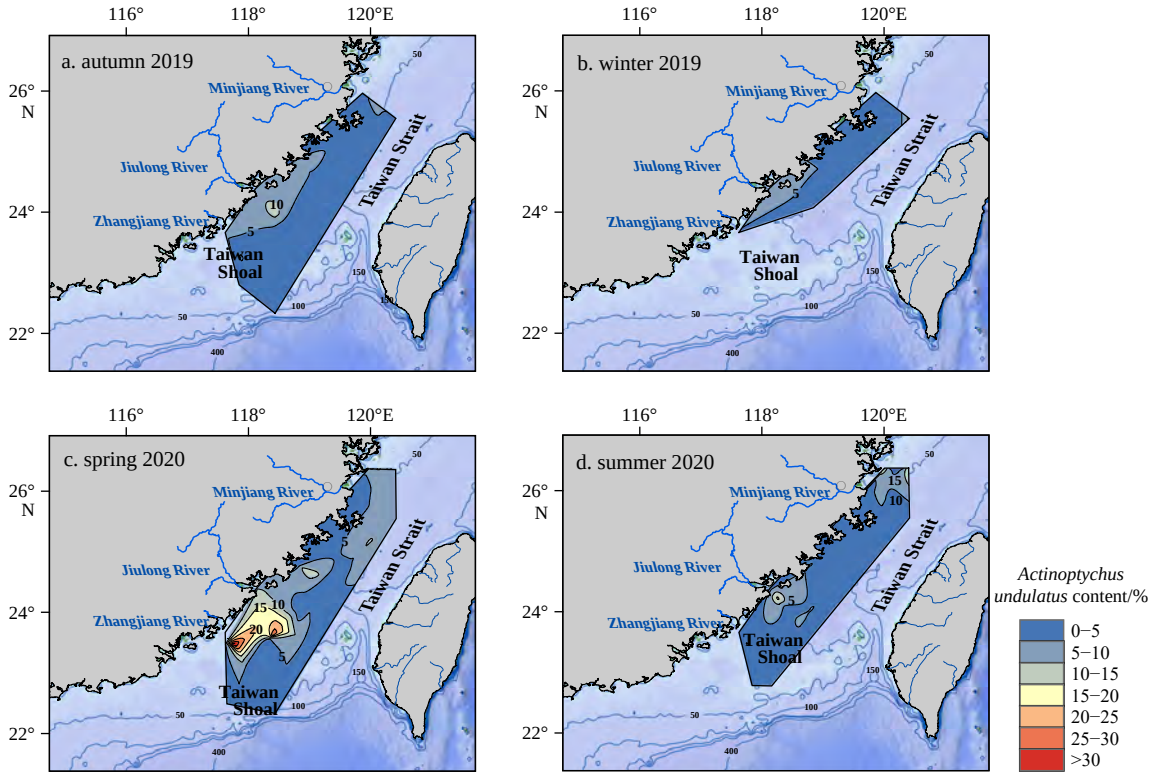


**Fig. 13.** Distribution of *Actinoptychus undulatus* in the Taiwan Strait: autumn 2019 (a), winter 2019 (b), spring 2020 (c), and summer 2020 (d).

*nodulifera*, *C. divisus*, and *Nitzschia brevissima* Grunow, each with content of 33.33%. The station was positively correlated with SSS, SST, and $NH_3$ (Fig. 17). The station reflected the emergence of a warm water species (i.e., *A. nodulifera*); therefore, the station

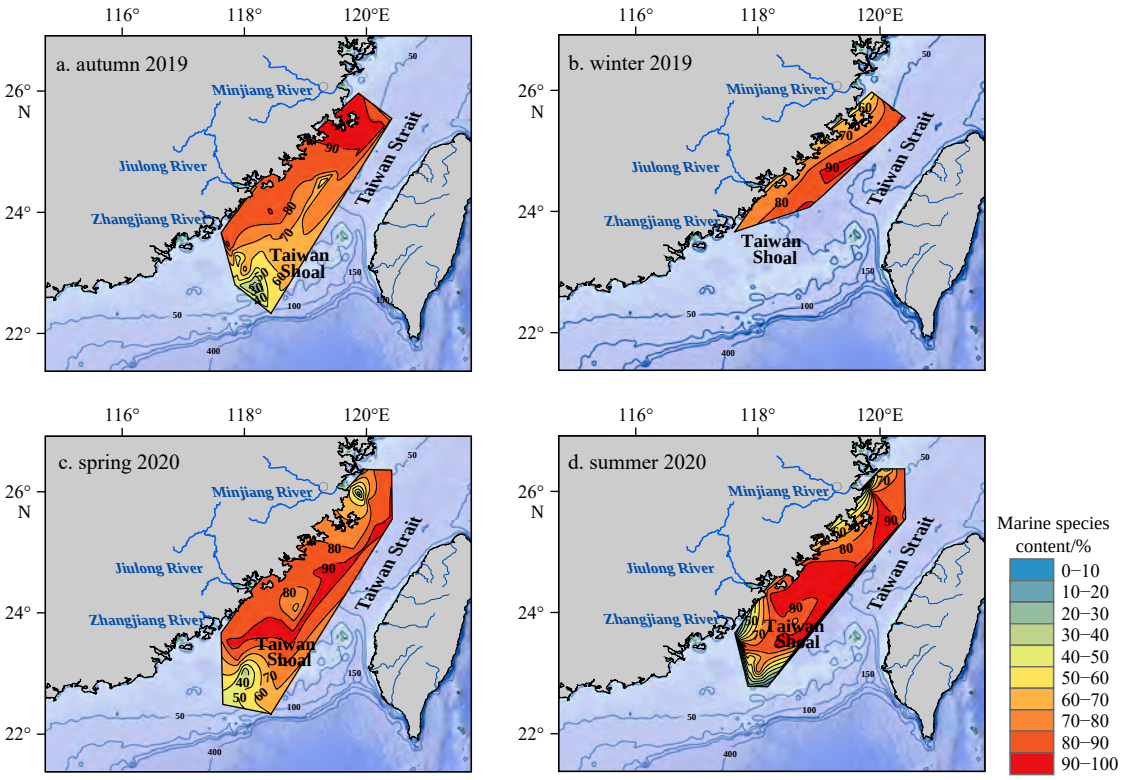


**Fig. 14.** Distribution of marine diatom species in the Taiwan Strait: autumn 2019 (a), winter 2019 (b), spring 2020 (c), and summer 2020 (d).

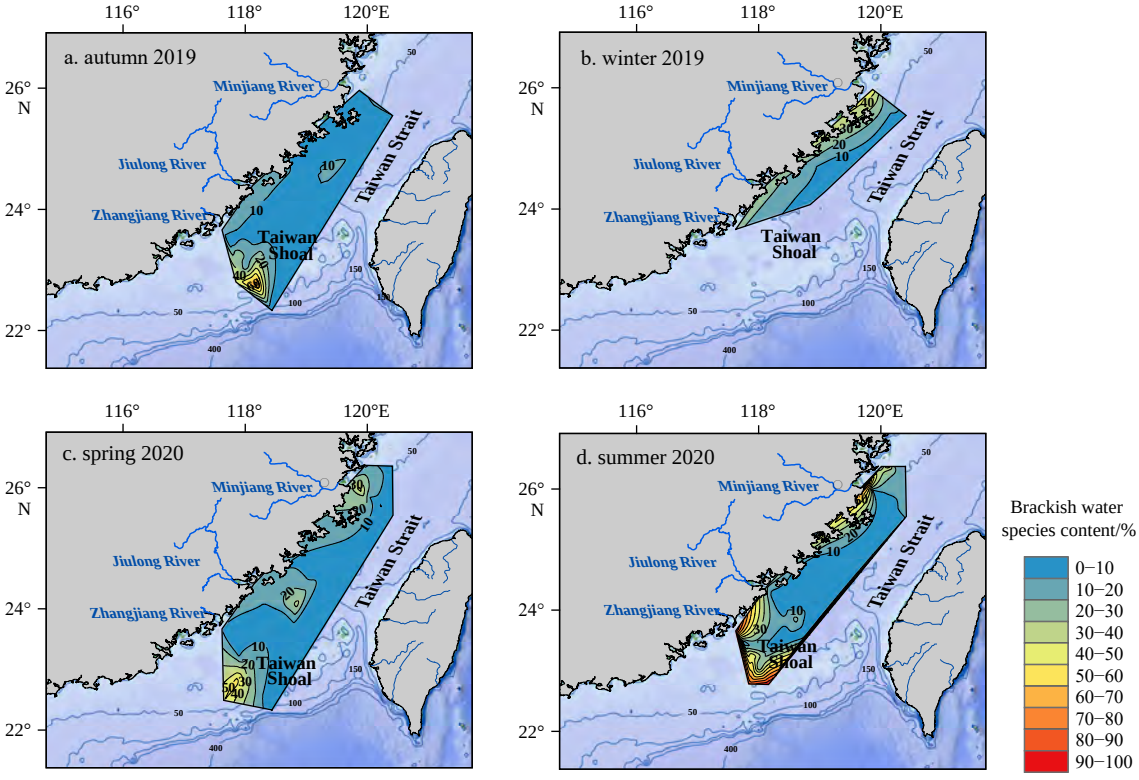


**Fig. 15.** Distribution of brackish water diatom species in the Taiwan Strait: autumn 2019 (a), winter 2019 (b), spring 2020 (c), and summer 2020 (d).

might reflect the influence of warm water. The station also reflected the emergence of a freshwater species (i.e., *N. brevissima*); therefore, the station might also reflect the influence of dilution by terrestrial rivers.

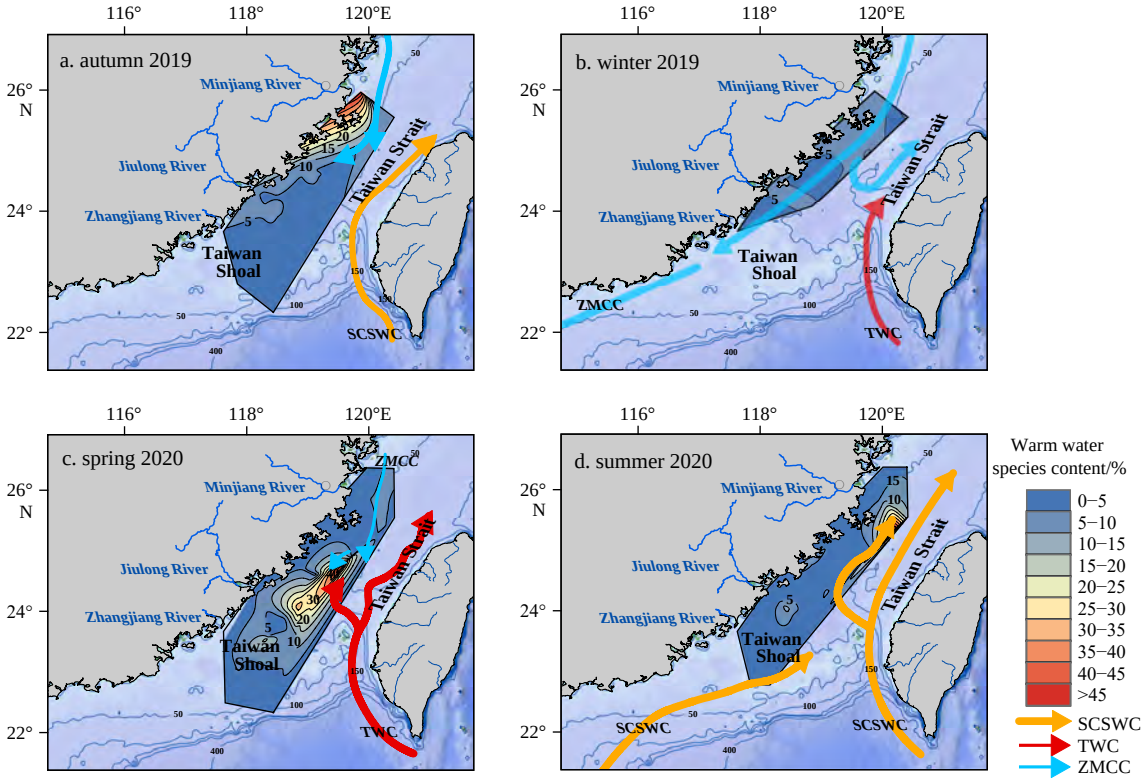


**Fig. 16.** Distribution of warm water diatom species in the Taiwan Strait: autumn 2019 (a), winter 2019 (b), spring 2020 (c), and summer 2020 (d).

**Table 2.** Summary of RDA results

| Axes | 1 | 2 | 3 | 4 | 5 | 6 | 7 | 8 | 9 | 10 |
|---|---|---|---|---|---|---|---|---|---|---|
| Eigenvalues | 0.059 14 | 0.033 28 | 0.016 01 | 0.013 96 | 0.009 92 | 0.001 04 | 0.005 91 | 0.003 83 | 0.003 59 | 0.002 30 |
| Proportion explained | 0.111 87 | 0.062 96 | 0.030 28 | 0.026 41 | 0.018 76 | 0.015 32 | 0.011 17 | 0.007 25 | 0.006 78 | 0.004 35 |
| Cumulative proportion | 0.111 87 | 0.174 83 | 0.205 11 | 0.231 52 | 0.250 28 | 0.265 60 | 0.276 78 | 0.284 03 | 0.290 82 | 0.295 17 |

## 5 Discussion

### 5.1 *Principal environmental factors affecting spatiotemporal diatom abundance and spatiotemporal variation of diatom distribution*

To explore the principal environmental factors that affected diatom abundance, Pearson correlation analysis was conducted on the diatom abundance and environmental factor data in this study (Table 4). Overall, the environmental factors of depth, SSS, Mz, Si, $NO_2^-$, $NO_3^-$, and $PO_4^{3-}$ had a greater effect on the change in diatom abundance in the study area than that of the factors of SST, DO, and $NH_3$.

In autumn 2019, the abundance of diatoms was affected by six environmental factors: $NO_3^-$, $PO_4^{3-}$, $NH_3$, $NO_2^-$, Si, and Mz, and it showed strong positive correlation with $NO_2^-$, Si, and Mz, indicating that the abundance of diatoms in this season was substantially controlled by nutrients. In autumn 2019, the abundance of diatoms in the coastal area, especially near the Jiulong River Estuary, was high (Fig. 9), which was broadly consistent with the areas of high values of nutrients. Biological activity in the study area was weak in autumn, and the ZMCC system (characterized by low salinity, low temperature, and high nutrient content) had a strong effect, leading to substantial increase in nutrient content along the western coast of the Taiwan Strait (Gu et al., 1992), which resulted in the higher abundance of diatoms. As a medium-sized river in the East Asian monsoon region, the Jiulong River discharges a large amount of terrestrial material into the Taiwan Strait owing to its large runoff. Additionally, human activities have discharged large volumes of nutrients into the Jiulong River over many years, resulting in the high nutrient content in the Jiulong River Estuary (Yan et al., 2012), which has created a good habitat for the growth of diatoms and accounts for the high diatom abundance in the Jiulong River Estuary. In this season, the particle size of the sediment in the estuary of each of the three main rivers in the study area was small (Fig. 3). The positive correlation between Mz and diatom abundance might also be caused by enrichment of diatoms and co-deposition of fine-grained material in the estuaries.

The abundance of diatoms both in winter 2019 and in spring 2020 was found correlated negatively with depth. Diatom abundance showed a trend of reduction from the coast to the open sea, which was most obvious in the western Taiwan Strait (Mao, 2020). In winter 2019, owing to insufficient sampling stations and data, the abundance of diatoms was not a true reflection owing to the influence of the ZMCC system. In spring 2020, the abundance of diatoms was also found correlated negatively with SSS. At this time, low abundance of diatoms was evident in the Taiwan Shoal area, which might reflect the strong hydrodynamic forces of the high-temperature high-salinity water that enter the Taiwan Shoal area in spring (Wan et al., 2013) and prevent *in situ* sedimentation of diatom valves.

In summer 2020, diatom abundance showed strong positive

**Table 3.** Characteristics of the dominant species in the different diatom assemblages

| Diatom assemblage | Dominating species | | Abundance range/% | Average abundance/% | Ecological habits |
|---|---|---|---|---|---|
| | Genus | Species | | | |
| Assemblage Ⅰ | *Actinoptychus* | *undulates* | 0–36.26 | 6.88 | Brackish species, common on coasts, benthonic, widespread in world seas (Jin et al., 1965, 1982; Guo and Qian, 2003 ) |
| | *Coscinodiscus* | *oculatus* | 0–31.11 | 6.70 | Temperate species (Jin et al., 1982; Guo and Qian, 2003) |
| | | *radiatus* | 0–18.37 | 4.95 | Widespread in world seas, warm water species, planktonic (Jin et al., 1982; Guo and Qian, 2003) |
| | *Paralia* | *sulcata* | 0–64.18 | 27.08 | Benthic species, typical shallow marine species, water depth of 50–100 m is most suitable for its growth (Jin et al., 1982; Hasle and Syvertsen, 1997; Guo and Qian, 2003; Zhang et al., 2016). Widely distributed in global offshore and upwelling water columns (Abrantes, 1988; Karpuz and Schrader, 1990; Lange et al., 1998; Abrantes et al., 2007). Low illumination and fairly low salinity (brackish water) (Blasco et al., 1980) |
| | *Podosira* | *stelliger* | 0–17.65 | 5.84 | Marine, benthic species (Jin et al., 1982; Guo and Qian, 2003) |
| | *Pyxidicula* | *weyprechtii* | 0–26.67 | 6.38 | Exotic planktonic species (Jin et al., 1982; Guo and Qian, 2003) |
| Assemblage Ⅱ | *Azpeitia* | *nodulifera* | 0–50 | 3.67 | Warm water species, benthic (Jin et al., 1982; Hasle and Syvertsen, 1997; Guo and Qian, 2003; Onodera et al., 2005; Ren et al., 2014) Common in the surface sediments of the equatorial and tropical Pacific (Jousé et al., 1971). Often distributed in the Kuroshio (Lan et al., 1995; Chen et al., 2014) |
| | *Coscinodiscus* | *rothii* | 0–100 | 23.50 | Marine or brackish species (Jin et al., 1982; Guo and Qian, 2003) |
| | *Cyclotella* | *striata* | 0–100 | 7.78 | Marine coastal species, planktonic species (Jin et al., 1982; Guo and Qian, 2003) |
| | *Paralia* | *sulcata* | 0–42.86 | 9.053 | – |
| | *Podosira* | *stelliger* | 0–50 | 7.69 | – |
| | *Trachyneis* sp. | | 0–17.65 | 2.68 | Marine benthic species, widely distributed (Jin et al., 1982) |
| Assemblage Ⅲ | *Coscinodiscus* | *rothii* | 0–35.14 | 3.63 | – |
| | *Paralia* | *sulcata* | 0–100 | 34.92 | – |
| | *Podosira* | *weyprechtii* | 0–100 | 12.26 | – |
| | *Pyxidicula* | *stelliger* | 0–33.33 | 8.87 | – |
| Assemblage Ⅳ | *Coscinodiscus* | *decrescens* | 0–50 | 25 | Rare species in coastal and intertidal zones (Jin et al., 1982; Guo and Qian, 2003) |
| | *Thalassiosira* | *eccentrica* | 50 | 50 | In addition to the Antarctic and Arctic, eurythermal and planktonic species are widely distributed in all oceans (Jin et al., 1965) |
| TS05 (spring 2020) | *Azpeitia* | *nodulifera* | 33.33 | 33.33 | – |
| | *Coscinodiscus* | *divisus* | 33.33 | 33.33 | Common on shores and intertidal in Fujian (Guo and Qian, 2003) |
| | *Nitzschia* | *brevissima* | 33.33 | 33.33 | Fresh or brackish species (Jin et al., 1982) |

Note: – represents no data.

**Table 4.** Pearson correlation analysis of diatom abundance and environmental variables

| | Depth | SST | SSS | DO | $NO_3^-$ | $PO_4^{3-}$ | $NH_3$ | $NO_2^-$ | $SiO_3^{2-}$ | Mz |
|---|---|---|---|---|---|---|---|---|---|---|
| 2019 Autumn | –0.377 | –0.104 | –0.326 | 0.161 | 0.514* | 0.523* | 0.440* | 0.596** | 0.625** | 0.676** |
| 2019 Winter | –0.647* | –0.112 | –0.168 | 0.034 | 0.125 | – | – | – | 0.221 | – |
| 2020 Spring | –0.522* | –0.211 | –0.557* | 0.343 | –0.018 | 0.158 | –0.007 | 0.17 | 0.192 | 0.406 |
| 2020 Summer | –0.306 | –0.204 | –0.046 | 0.228 | –0.109 | 0.235 | –0.135 | 0.35 | 0.38 | 0.603** |

Note: *significant correlation ($p < 0.05$), **significant correlation ($p < 0.01$); SSS, sea surface salinity; SST, sea surface temperature; Mz, mean grain size; DO, dissolved oxygen; $SiO_3^{2-}$, silicate; $NO_2^-$, nitrite; $NO_3^-$, nitrate; $PO_4^{3-}$, phosphate; $NH_3$ – ammonia nitrogen.

correlation with Mz. The northern part of the study area is in the Zhejiang–Fujian area of mud deposition (Liu et al., 2006) with a smaller sediment particle size (Fig. 3). Diatoms were easily enriched in the fine-grained sediments. Therefore, the highest values of diatom abundance in this season appeared in the northern part of the study area.

In autumn 2019, Assemblage Ⅰ, which represents a coastal environment, was concentrated in the sea area outside the estuaries of the Minjiang River, Jiulong River, and Zhangjiang River. Assemblage Ⅱ, containing warm water species, appeared in the Taiwan Shoal area, indicating that the area was affected by warm water. Assemblage Ⅲ, which contains exotic species, was distributed parallel to the coast in the central Taiwan Strait. By winter 2019, the distribution range of Assemblage Ⅲ was notably smaller, remaining scattered only in the middle and north of the study area. Assemblage Ⅲ was covered by Assemblage Ⅰ, showing that the population of exotic species decreased in winter 2019 in comparison with that in autumn.

In spring 2020, the distribution of Assemblage Ⅱ, representing the warm water coastal environment, increased markedly both in the Taiwan Shoal area and in the northern part of the study area in comparison with that in autumn 2019, indicating that large volumes of warm water entered those sea areas during this season. In summer 2020, both Assemblage Ⅱ and Assemblage Ⅲ showed a trend of expansion shoreward, and Assemblage Ⅲ became the most widely distributed diatom assemblage in this season. This reflects the large volume of warm water and large number of exotic species carried into the Taiwan

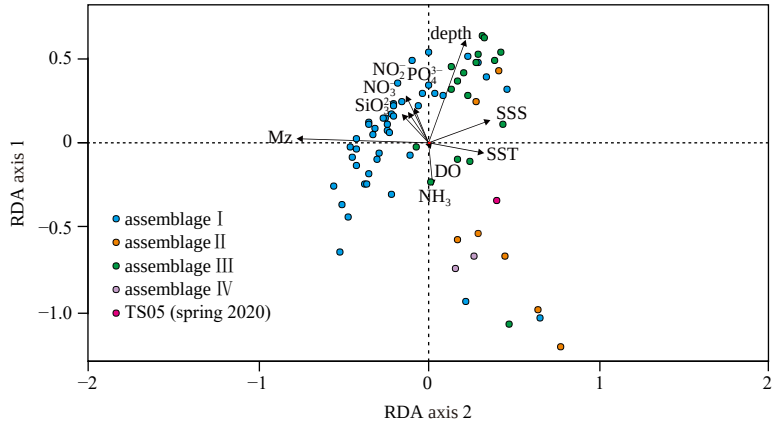


**Fig. 17.** RDA biplot of environmental variables and samples. The eigenvalue for RDA axis 1 and 2 is 0.059 and 0.033, respectively. Abbreviations: SSS, sea surface salinity; SST, sea surface temperature; Mz, mean grain size; DO, dissolved oxygen; $SiO_3^{2-}$, silicate; $NO_2^-$, nitrite; $NO_3^-$, nitrate; $PO_4^{3-}$, phosphate; $NH_3$, ammonia nitrogen. Assemblages Ⅰ–Ⅳ and TS05 were analyzed by cluster analysis, and samples were labeled with different colors.

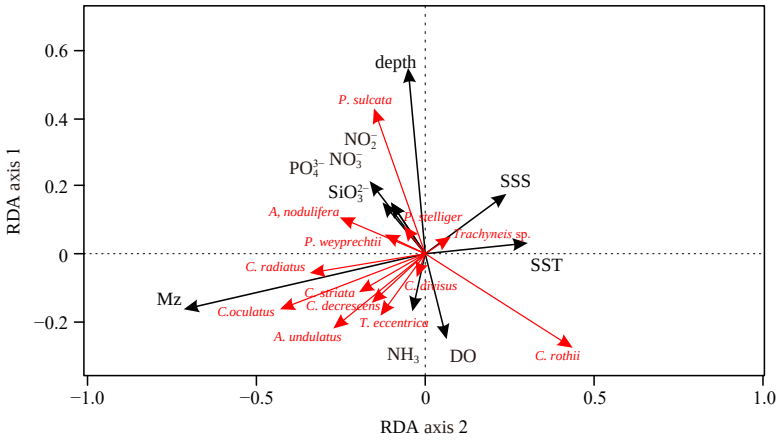


**Fig. 18.** RDA biplot of diatom taxa and environmental factors. Abbreviations: SSS, sea surface salinity; SST, sea surface temperature; Mz, mean grain size; DO, dissolved oxygen; $SiO_3^{2-}$, silicate; $NO_2^-$, nitrite; $NO_3^-$, nitrate; $PO_4^{3-}$, phosphate; $NH_3$, ammonia nitrogen. *P. sulcata, Paralia sulcata*; *P. weyprechtii, Pyxidicula weyprechtii; P. stelligera, Podosira stelligera; A. nodulifera, Azpeitia nodulifera; C. radiatus, Coscinodiscus radiatus; C. oculatus, Coscinodiscus oculatus; C. striata, Cyclotella striata; A. undulatus, Actinoptychus undulatus; C. decrescens, Coscinodiscus decrescens; T. eccentrica, Thalassiosira eccentrica; C. divisus, Coscinodiscus divisus; C. rothii, Coscinodiscus rothii;*

Strait by the strong SCSWC in summer 2020, which also restricted the range of Assemblage Ⅰ to patchy distribution in the north of the study area. Controlled by the East Asian monsoon, rivers in southeastern China flood in spring and summer every year (Wang et al., 2022).

In the spring and summer of 2020, the content of freshwater species in the Taiwan Shoal area was high, which might reflect enhancement of dilution by Zhujiang River water that affected the characteristics of the water mass in the southern part of the study area and formed some low-salinity areas in the Taiwan Shoal.

A separate group (Station TS05) also appeared in spring 2020, and its characteristic of high content of freshwater species differed markedly from that of surrounding stations. This reflects that the station might have been affected by freshwater input from rivers. However, the absence of freshwater species at other stations closer to the Jiulong River Estuary indicates that the freshwater species at this station may have been transported from other places.

### 5.2 *Response of diatom distribution to ocean currents*

Previous studies showed that the intensity of the seasonal intrusion of the TWC into the Taiwan Strait reduces in the order of spring > winter > summer > autumn (Sun, 2016). In spring, owing to gradual weakening of the northeast winter monsoon forcing and reduction in the forcing of the East Asian Monsoon, the TWC drives further north, and it reaches its peak intensity in April–May, when the TWC water body with high temperature and high salinity dominates the entire Taiwan Strait (Sun, 2016).

In spring 2020, the content of warm water species in the study area was significantly higher than that in other seasons (Fig. 12), and Assemblage Ⅱ expanded northward to central and northern parts of the study area, all of which were related to strengthening of the TWC forcing during that season. The main warm water species in the study area (i.e., *A. nodulifera*) were found to be significantly negatively correlated with SST (Fig. 11) but were consistent with the area of flow of the TWC. Thus, those species were not produced by *in situ* water bodies, but were carried by ocean currents and then sedimented. In summer, the southwest sum-

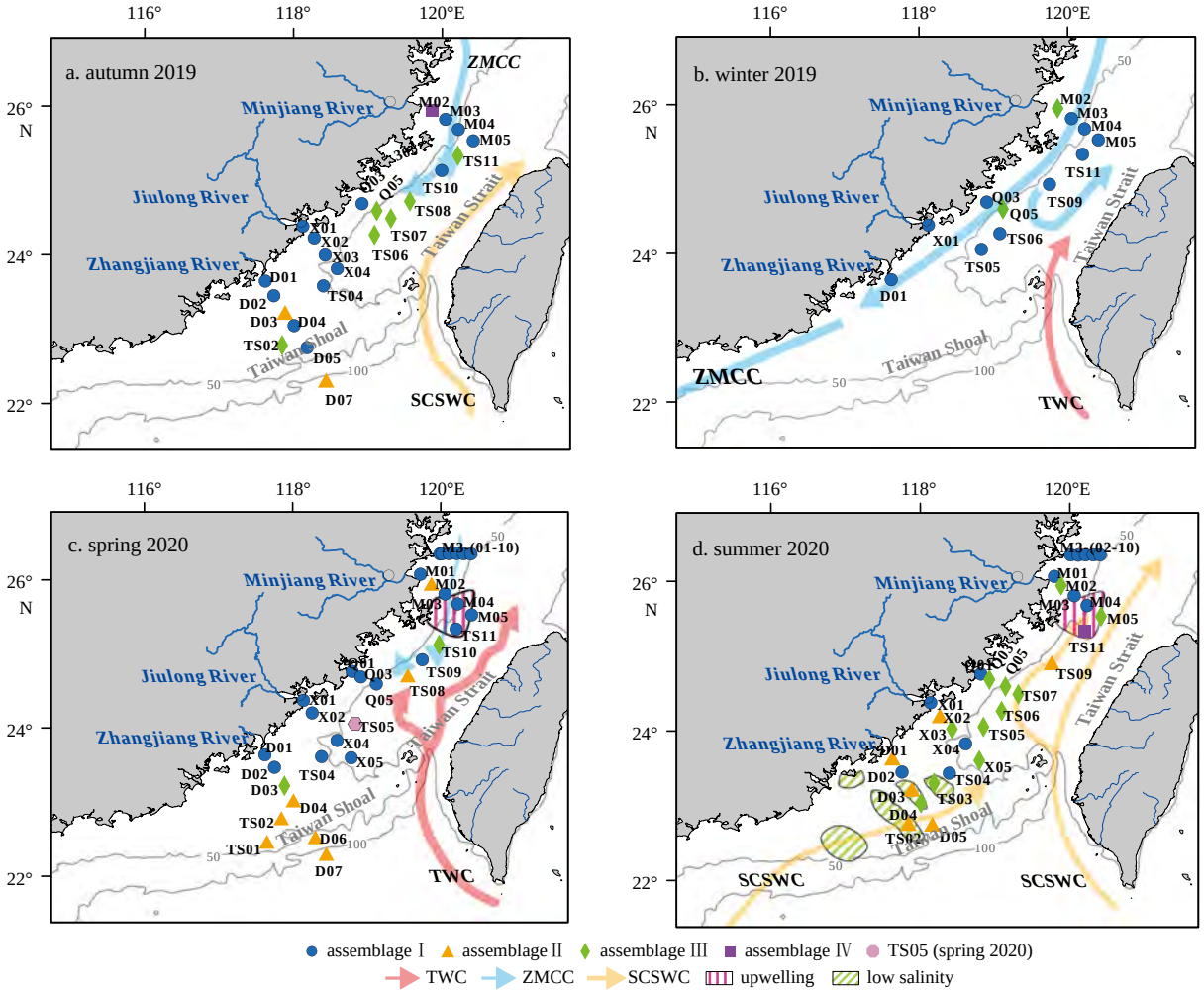


**Fig. 19.** Distribution of diatom assemblages in the Taiwan Strait: autumn 2019 (a), winter 2019 (b), spring 2020 (c), and summer 2020 (d). Red arrows represent the Taiwan Warm Current (TWC), blue arrows represent the Zhejiang-Fujian Coastal Current (ZMCC) system, and yellow arrows represent the South China Sea Warm Current (SCSWC).

mer monsoon is dominant, SCS water invades through the PHC, and TWC water is replaced by high-temperature low-salinity SCS water (Jan et al., 2002). Consequently, Assemblage Ⅲ was found distributed over a large area in central and southern parts of the study area (Fig. 19d), and a high-value area of warm water species related to the strong invasion of SCS water formed in the area offshore of the Minjiang River Estuary (Fig. 12d). The succession of these diatom assemblages indicate change in the range of influence of the warm currents.

In autumn, the diatom assemblage on the western side of the Taiwan Strait comprised mainly Assemblage Ⅰ, representing a coastal population. The distribution of warm water species was compressed into the southeast of the region, indicating that the influence of the ZMCC was enhanced and that of the SCSWC was weakened. In autumn, the diatom abundance at Station M02 in the Minjiang River Estuary was extremely low. This might reflect the influence of the ZMCC and the Minjiang River runoff in forming an area with high turbidity that affected the growth and sedimentation of diatoms (Meng and Xu, 2013).

In winter, the strong northeast winter monsoon pushed the low-temperature low-salinity ZMCC southward and prevented northward incursion of the TWC. These two opposing currents collided near the PHC, forming ocean peaks (Li et al., 2000, 2006; Chang et al., 2006; Sun, 2016). The ZMCC flowed southward under the backing of the TWC, and some water bodies turned back from the south to the north to form a U-type current (Oey et al., 2014). The high-value area of warm water species in the northeast of the study area in this season was the result of the mixing and transportation of this ocean current water body (Fig. 12b).

In summary, TWC and SCSWC brought abundant warm-water diatoms to the Taiwan Strait. The ZMCC converged with these warm currents in the north-central Taiwan Strait, resulting in a top-up effect, thus forming a high-value area of warm water species.

### 5.3 *Effect of upwelling on diatom distribution*

To the south of the Minjiang River Estuary, the effect of seawater dynamics is strong and upwelling is substantial. The upwelling is most active from May to July, and it declines at the end of August (Tang et al., 2002, 2004; Fan et al., 2012). The sub-high-value area of diatom abundance in this area in the spring and summer of 2020 (Fig. 9) coincided with the time of upwelling, suggesting that the increase in diatom abundance was caused by the upwelling of nutrient-rich deep water to the sea surface (Shen and Shi, 2002). Some earlier studies reported that diatom abundance at the boundary of the area of upwelling is very low (Yang, 1995; Fan et al., 2012). In summer 2020, diatom abundance was extremely low in the northern part of the study area at Station

TS11, located at the boundary of the upwelling system.

Therefore, the diatom fossil assemblages could reflect the variation of the warm current in the Taiwan Strait in geological history. They can be used to reveal the changes of paleocurrent and paleoclimate in Taiwan Strait.

## 6 Conclusions

In this study, the distribution of diatoms in the surface sediments of the Taiwan Strait was investigated, and the spatiotemporal changes in diatoms and their response to ocean currents were analyzed. The main conclusions are as follows.

(1) Overall, 44 genera and 118 species (including species and varieties) of diatom were identified in the surface sediments from autumn 2019 to summer 2020. Total diatom abundance was 8–27 353 valves/g with an average value of 2 459 valves/g. Diatom species were mainly marine species, and there were 16 dominant species. The content of warm water species was also relatively high, especially that of *A. nodulifera*. Freshwater species were also scattered in areas such as the Taiwan Shoals and the estuaries of bordering rivers.

(2) Four assemblages were identified that represented different marine environments. Assemblage Ⅰ represented a coastal environment. Assemblage Ⅱ represented a coastal environment affected by warm water. Assemblage Ⅲ represented a coastal environment that was substantially affected by the ocean. The diatom abundance of Assemblage Ⅳ was extremely low.

(3) The abundance of diatoms in different times was controlled by different environmental factors. In autumn 2019, the principal controlling factors were nutrients and particle size. In winter 2019, diatom abundance was affected mainly by water depth. In spring 2020, the controlling factors were primarily water depth and SSS, whereas particle size was the principal controlling factor of diatom abundance in summer 2020. Additionally, in autumn 2019, diatom abundance was also affected by human activities, and the highest value appeared in the Jiulong River Estuary. Overall, diatom abundance decreased from the coast toward the open sea.

(4) In winter 2019, Assemblage Ⅲ (*P. sulcata, P. weyprechtii, P. stelliger, C. rothii*) was covered by Assemblage Ⅰ (*P. sulcata, A. undulatus, C. oculatus, P. weyprechtii, P. stelliger, C. radiatus*) owing to reduction in the population of exotic diatom species in comparison with that in autumn 2019, and Assemblage Ⅲ was found distributed sporadically only in central and northern parts of the study area. In spring 2020, a large volume of warm water intruded into the Taiwan Shoal and northern part of the study area, and the distribution of Assemblage Ⅱ (*C. rothii, P. sulcata, C. striata, P. stelliger, A. nodulifera, Trachyneis* sp.) increased markedly in comparison with that in autumn 2019. In summer 2020, the strong SCSWC transported large numbers of warm water and exotic diatom species into the Taiwan Strait, and Assemblage Ⅱ and Assemblage Ⅲ both showed a trend of coastal expansion. Spatiotemporal variation in diatom abundance in the surface sediments of the Taiwan Strait was strong, especially in spring and summer.

(5) The study area is mainly affected by the northward-flowing TWC and SCSWC and the cold ZMCC system. In spring and summer 2020, the TWC and SCSWC were strong, which led to expansion in the distribution of Assemblage Ⅱ and Assemblage Ⅲ, and corresponding high-value areas of warm water species appeared. In autumn and winter 2019, the ZMCC system was strong, supported by the northward TWC that formed a U-type flow in winter. Under the influence of the mixing and transportation of ocean current water, the content of warm water species in the northeast of the study area increased. Upwelling also had considerable influence on diatom abundance in the northern part of the study area. In summary, we believe that the succession of diatom assemblages reflects change in the range of influence of the warm currents.

(6) The surface sediment diatoms in the Taiwan Strait were affected by various environmental factors such as hydrodynamics, currents, salinity, and nutrients. Current and water mass systems are the most important factors in affecting the distribution of diatoms. Therefore, the diatoms in sediment cores could provide a basis for revealing changes of paleo current and water mass systems in the Taiwan Strait in the future under the premise of further verification.

***Acknowledgements***

We thank all the participants who helped us obtain samples and data during the voyages involved in this study, as well as the crew of the China Maritime Surveillance 203. We thank James Buxton MSc from Liwen Bianji (Edanz) (www.liwenbianji.cn/) for editing the English text of a draft of this manuscript.

## References

Abrantes F. 1988. Diatom assemblages as upwelling indicators in surface sediments off Portugal. Marine Geology, 85(1): 15–39, doi: 10.1016/0025-3227(88)90082-5

Abrantes F, Lopes C, Mix A, et al. 2007. Diatoms in Southeast Pacific surface sediments reflect environmental properties. Quaternary Science Reviews, 26(1–2): 155–169, doi: 10.1016/j.quascirev.2006.02.022

Armbrust E V. 2009. The life of diatoms in the world's oceans. Nature, 459(7244): 185–192

Blasco D, Estrada M, Jones B. 1980. Relationship between the phytoplankton distribution and composition and the hydrography in the northwest African upwelling region near Cabo Corbeiro. Deep-Sea Research Part A: Oceanographic Research Papers, 27(10): 799–821

Chang Yi, Shimada T, Lee Ming-An, et al. 2006. Wintertime sea surface temperature fronts in the Taiwan Strait. Geophysical Research Letters, 33(23): L23603

Chang Yuan-Pin, Wang Wei-Lung, Chen Min-Te. 2009. The last 100 000 years' palaeoenvironmental changes inferred from the diatom assemblages of core MD012404 from the Okinawa Trough, East China Sea. Journal of Quaternary Science, 24(8): 890–901

Chen Zhaozhang, Hu Jianyu, Zhu Jia, et al. 2008. Observation of upwelling and diluted water in southern Taiwan Strait during July, 2005. Journal of Tropical Oceanography (in Chinese), 27(4): 19–22

Chen Min, Lan Binbin, Shen Linnan, et al. 2014. Characteristics of diatom distribution in the surface sediments of the Western Philippine Basin. Acta Micropalaeontologica Sinica (in Chinese), 31(4): 321–334

Chen Min, Li Yunhai, Qi Hongshuai, et al. 2019. The influence of season and Typhoon Morakot on the distribution of diatoms in surface sediments on the inner shelf of the East China Sea. Marine Micropaleontology, 146: 59–74, doi: 10.1016/j.marmicro.2019.01.003

Chen Min, Qi Hongshuai, Intasen W, et al. 2020. Distributions of diatoms in surface sediments from the Chanthaburi coast, Gulf of Thailand, and correlations with environmental factors. Regional Studies in Marine Science, 34: 100991, doi: 10.1016/j.rsma.2019.100991

Chen Min, Qi Hongshuai, Lan Dongzhao, et al. 2016. Paleoenvironmental evolution of the Beilun River estuary, northwest South China Sea, during the past 20, 000 years based on diatoms. Acta Geologica Sinica: English Edition, 90(6): 2244–2257, doi: 10.1111/1755-6724.13034

Chen Min, Qi Hongshuai, Shen Linnan, et al. 2022. Research pro-

gress of microorganisms from marine storm deposits. Journal of Applied Oceanography (in Chinese), 41(3): 516–523
Chen Chun, Zhao Guangtao, Chen Min, et al. 2012. Diatom assemblages in coastal surface sediments in southeast of China. Marine Geology & Quaternary Geology (in Chinese), 32(2): 109–114
Cheng Zhaodi, Gao Yahui, Dickman M. 1996. Colour Plates of the Diatoms (in Chinese). Beijing: China Ocean Press, 1–120
Edwards S, McKirdy D M, Bone Y, et al. 2006. Diatoms and ostracods as mid-Holocene palaeoenvironmental indicators, North Stromatolite Lake, Coorong National Park, South Australia. Australian Journal of Earth Sciences, 53(4): 651–663, doi: 10.1080/08120090600686801
Fan Yanbin, Li Chao, Wu Xiang'en. 2012. Effect of southeast coastal upwelling in Haitan Island of northwestern Taiwan Strait on surface sedimentary diatom. Journal of Anhui Agricultural Sciences (in Chinese), 40(1): 363–366
Folk R L, Ward W C. 1957. Brazos River bar [Texas]; a study in the significance of grain size parameters. Journal of Sedimentary Research, 27(1): 3–26, doi: 10.1306/74D70646-2B21-11D7-8648000102C1865D
Gu Deyu, Chen Lianzhi, Guo Shuihuo. 1992. Temporal and spacial variations of nutrients in western part of Taiwan Strait and their relations to hydrological and biological factors. Journal of Tropical Oceanography (in Chinese), 11(1): 96–100
Guo Yujie, Qian Shuben. 2003. Flora Algarum Marinarum Sinicarum (in Chinese). Beijing: Science Press, 1–493
Håkansso H. 1984. The recent diatom succession of Lake Havgårdssjön, South Sweden. In: Mann D G, ed. Proceedings of the 7th International Diatom Symposium. Koenigstein: Otto Koeltz Science Publishers, 411–429
Hasle G R, Syvertsen E E. 1997. Marine diatoms. In: Tomas C R, ed. Identifying Marine Phytoplankton. San Diego: Academic Press, 5–385
Hong Huasheng, Zhang Caiyun, Shang Shaoling, et al. 2009. Interannual variability of summer coastal upwelling in the Taiwan Strait. Continental Shelf Research, 29(2): 479–484, doi: 10.1016/j.csr.2008.11.007
Horng Chorng-Shern, Huh Chih-An. 2011. Magnetic properties as tracers for source-to-sink dispersal of sediments: a case study in the Taiwan Strait. Earth and Planetary Science Letters, 309(1–2): 141–152
Hu Yi. 2011. Sediment characters and major river contribution to the west side nearshore of the Taiwan Strait (in Chinese)[dissertation]. Qingdao: Ocean University of China
Hu Yi, Jia Ruzhen, Xu Jiang, et al. 2022. Research advance and prospect of tidal sands in Taiwan Strait. Journal of Applied Oceanography (in Chinese), 41(3): 500–515
Hu Jun, Lan Wenlu, Huang Bangqin, et al. 2015. Low nutrient and high chlorophyll *a* coastal upwelling system—a case study in the southern Taiwan Strait. Estuarine, Coastal and Shelf Science, 166: 170–177
Huh Chih-An, Chen Weifang, Hsu Feng-Hsin, et al. 2011. Modern (<100 years) sedimentation in the Taiwan Strait: rates and source-to-sink pathways elucidated from radionuclides and particle size distribution. Continental Shelf Research, 31(1): 47–63, doi: 10.1016/j.csr.2010.11.002
Jan Sen, Wang Joe, Chern Ching-Sheng, et al. 2002. Seasonal variation of the circulation in the Taiwan Strait. Journal of Marine Systems, 35(3–4): 249–268, doi: 10.1016/S0924-7963(02)00130-6
Jiang Hui. 1987. Environment analysis of the common fossil diatoms from the sediments of China Sea. Acta Botanica Sinica (in Chinese), 29(4): 440–448
Jin Dexiang. 1982. Ecological studies on diatoms from Taiwan Strait. Taiwan Strait (in Chinese), 1(1): 80–86
Jin Dexiang, Chen Jinhuan, Huang Kaige. 1965. Planktonic Diatoms of China Seas (in Chinese). Shanghai: Shanghai Science and Technology Press, 1–229
Jin Dexiang, Cheng Zhaodi, Lin Junmin, et al. 1982. Benthic Diatoms of China Seas (in Chinese). Beijing: China Ocean Press, 1–323
Jin Dexiang, Cheng Zhaodi, Liu Shicheng, et al. 1992. Benthic Diatoms of China Seas (in Chinese). Beijing: China Ocean Press, 1–437
Jousé A P, Kozlova O G, Muhina V V. 1971. Distribution of diatoms in the surface layer of sediment from the Pacific Ocean. In: Funnell B M, Riedel W R, eds. The Micropalaeontology of Oceans. London: Cambridge University Press, 263–269
Kang Jianhua, Lin Yili, Huang Shuhong, et al. 2020. Size-fractionated biomass of phytoplankton and its environmental impact factors in the waters off northwestern Xiamen Island. Ocean Development and Management (in Chinese), 37(12): 54–62
Karpuz N K, Schrader H. 1990. Surface sediment diatom distribution and Holocene paleotemperature variations in the Greenland, Iceland and Norwegian Sea. Paleoceanography, 5(4): 557–580
Lan Dongzhao. 1989. Diatoms and silicoflagellates distribution in surface sediment of western Taiwan Strait. Journal of Oceanography in Taiwan Strait (in Chinese), 8(4): 322–328
Lan Dongzhao, Cheng Zhaodi, Liu Shicheng. 1995. Late Quaternary diatom remains in South China Sea and their geological significance Ⅷ. Discussion on some problems. Journal of Oceanography in Taiwan Strait (in Chinese), 14(3): 235–240
Lange C B, Romero O E, Wefer G, et al. 1998. Offshore influence of coastal upwelling off Mauritania, NW Africa, as recorded by diatoms in sediment traps at 2 195 m water depth. Deep-Sea Research Part I: Oceanographic Research Papers, 45(6): 985–1013, doi: 10.1016/S0967-0637(97)00103-9
Li Li, Guo Xiaogang, Wu Risheng. 2000. Oceanic fronts in southern Taiwan Strait. Journal of Oceanography in Taiwan Strait (in Chinese), 19(2): 147–156
Li Chunyan, Hu Jianyu, Jan S, et al. 2006. Winter-spring fronts in Taiwan Strait. Journal of Geophysical Research: Oceans, 111(C11): C11S13
Liu JinPu Paul, Li Anchun, Xu Kehui, et al. 2006. Sedimentary features of the Yangtze River-derived along-shelf clinoform deposit in the East China Sea. Continental Shelf Research, 26(17–18): 2141–2156, doi: 10.1016/j.csr.2006.07.013
Liu Zhongcheng, Liu Baohua, Huang Zhenzhong, et al. 2005. Topography and Geomorphology of China's Offshore and Adjacent Waters (in Chinese). Beijing: China Ocean Press, 1–227
Mao Jianfei. 2020. Diatoms in sediment of Taiwan Strait and their environmental indications (in Chinese)[dissertation]. Xiamen: Xiamen University
Meng Zhaocui, Xu Kuidong. 2013. Ecological characteristics of benthic diatoms, protozoa and meiobenthos in the sediments of the Changjiang Estuary and East China Sea in spring. Acta Ecologica Sinica (in Chinese), 33(21): 6813–6824, doi: 10.5846/stxb201207090964
Milliman J D, Lin S W, Kao S J, et al. 2007. Short-term changes in seafloor character due to flood-derived hyperpycnal discharge: typhoon Mindulle, Taiwan, July 2004. Geology, 35(9): 779–782
Nakamura H, Okazaki Y, Konno S, et al. 2020. An assessment of diatom assemblages in the Sea of Okhotsk as a proxy for sea-ice cover. Journal of Micropalaeontology, 39(1): 77–92, doi: 10.5194/jm-39-77-2020
Oey L Y, Chang Y L, Lin Y C, et al. 2014. Cross flows in the Taiwan Strait in winter. Journal of Physical Oceanography, 44(3): 801–817, doi: 10.1175/JPO-D-13-0128.1
Onodera J, Takahashi K, Honda M C. 2005. Pelagic and coastal diatom fluxes and the environmental changes in the northwestern North Pacific during December 1997–May 2000. Deep-Sea Research Part II: Topical Studies in Oceanography, 52(16–18): 2218–2239, doi: 10.1016/j.dsr2.2005.07.005
Pokras E M, Molfino B. 1986. Oceanographic control of diatom abundances and species distributions in surface sediments of the tropical and southeast Atlantic. Marine Micropaleontology, 10(1–3): 165–188
Ran Lihua, Zheng Yulong, Chen Jianfang, et al. 2011. The influence of monsoon on seasonal changes of diatom fluxes in the northern and central South China Sea. Haiyang Xuebao (in Chinese), 33(5): 139–145
Ren Jian, Gersonde R, Esper O, et al. 2014. Diatom distributions in northern North Pacific surface sediments and their relation-

ship to modern environmental variables. Palaeogeography, Palaeoclimatology, Palaeoecology, 402: 81–103
Shen Guoying, Shi Bingzhang. 2002. Marine Ecolog (in Chinese). 2nd ed. Beijing: Science Press, 1–446
Stoermer E F, Smol J P. 1999. The Diatoms: Applications for the Environmental and Earth Sciences. Cambridge: Cambridge University Press, 3–8
Sun Haowei, 2016. Seasonal and inter-annual variation of Kuroshio intrusion into the Taiwan Strait and its physical mechanisms (in Chinese)[dissertation]. Xiamen: Third Institute of Oceanography, Ministry of Natural Resources
Tang Danling, Kawamura H, Guan L. 2004. Long-time observation of annual variation of Taiwan Strait upwelling in summer season. Advances in Space Research, 33(3): 307–312, doi: 10.1016/S0273-1177(03)00477-0
Tang Danling, Kester D R, Ni I-Hsun, et al. 2002. Upwelling in the Taiwan Strait during the summer monsoon detected by satellite and shipboard measurements. Remote Sensing of Environment, 83(3): 456–471
Tao Shuqin, James T. Liu, Wang Aijun, et al. 2022. Deciphering organic matter distribution by source-specific biomarkers in the shallow Taiwan Strait from a source-to-sink perspective. Frontiers in Marine Science, 9: 969461, doi: 10.3389/fmars.2022.969461
Ter Braak C J F, Prentice I C. 1988. A theory of gradient analysis. In: Caswell H, ed. Advances in Ecological Research. Amsterdam: Elsevier, 271–317
Tréguer P, Bowler C, Moriceau B, et al. 2018. Influence of diatom diversity on the ocean biological carbon pump. Nature Geoscience, 11(1): 27–37, doi: 10.1038/s41561-017-0028-x
Wan Xiaofang, Pan Aijun, Guo Xiaogang, et al. 2013. Seasonal variation features of the hydrodynamic environment in the western Taiwan Strait. Journal of Applied Oceanography (in Chinese), 32(2): 156–163
Wang Kaifa, Jiang Hui, Zhang Yulan. 1990. Analysis of quaternary palynology and algae and environment in the South China Sea and the coastal area (in Chinese). Shanghai: Tongji University Press
Wang Yu, Kang Jianhua, Ye Youyin, et al. 2016. Phytoplankton community and environmental correlates in a coastal upwelling zone along western Taiwan Strait. Journal of Marine Systems, 154: 252–263, doi: 10.1016/j.jmarsys.2015.10.015
Wang Lihui, Zhong Haolin, Yu Zhiming, et al. 2022. Analysis of the runoff variation characteristics in the downstream of Minjiang River from 1950 to 2019. Journal of Fuzhou University: Natural Science Edition (in Chinese), 50(5): 681–686
Xiao Hui, Guo Xiaogang, Wu Risheng. 2002. Summarization of studies on hydrographic characteristics in Taiwan Strait. Journal of Oceanography in Taiwan Strait (in Chinese), 21(1): 126–138
Xu Yonghang, Chen Jian, Wang Aijun, et al. 2013. Clay minerals in surface sediments of the Taiwan Strait and their provenance. Acta Sedimentologica Sinica (in Chinese), 31(1): 120–129
Xu Zhifeng, Wang Mingliang, Hong Ashi, et al. 1989. Ages of sediments and sedimentation rates of the western Taiwan Strait since late Pleistocene. Journal of Oceanography in Taiwan Strait (in Chinese), 8(2): 114–121
Yan Xiuli, Zhai Weidong, Hong Huasheng, et al. 2012. Distribution, fluxes and decadal changes of nutrients in the Jiulong River Estuary, Southwest Taiwan Strait. Chinese Science Bulletin, 57(18): 2307–2318
Yang Qingliang. 1995. Species composition and distribution of planktonic diatoms in the west side of Taiwan Strait. Haiyang Xuebao (in Chinese), 17(2): 99–107
Zeng Xiangying, Liu Yi, Xu Liang, et al. 2021. Co-occurrence and potential ecological risk of parent and oxygenated polycyclic aromatic hydrocarbons in coastal sediments of the Taiwan Strait. Marine Pollution Bulletin, 173: 113093, doi: 10.1016/j.marpolbul.2021.113093
Zhang Jinpeng. 2009. Study on sedimentary diatoms of Late Holocene from middle offshore sea area of Fujian Province (in Chinese)[dissertation]. Xiamen: Xiamen University
Zhang Jinpeng, Tomczak M, Li Chao, et al. 2016. Significance of the *Paralia sulcata* fossil record in palaeoenvironmental reconstructions of the SE Asia marginal seas over the Last Glacial Cycle. Geological Society, London, Special Publications, 429(1): 211–221